International Journal of Mining Science and Technology xxx (xxxx) xxx

Contents lists available at ScienceDirect

International Journal of Mining Science and Technology

journal homepage: www.elsevier.com/locate/ijmst

Advances in thermo-hydro-mechanical-chemical modelling for CO_2 geological storage and utilization

Nanlin Zhang [a,b], Liangliang Jiang [c,*], Fushen Liu [b,*], Yuhao Luo [b], Lele Feng [d], Yiwen Ju [e], Allegra Hosford Scheirer [f], Jiansheng Zhang [g], Birol Dindoruk [h], SM Farouq Ali [h], Zhangxin Chen [c,i]

[a] School of Civil Engineering and Geomatics, Southwest Petroleum University, Chengdu 610500, China
[b] Research Center of Coastal and Urban Geotechnical Engineering, College of Civil Engineering and Architecture, Zhejiang University, Hangzhou 310058, China
[c] Department of Chemical and Petroleum Engineering, University of Calgary, Calgary T2N 1N4 Canada
[d] School of Safety Engineering, China University of Mining and Technology, Xuzhou 221116 China
[e] State Key Laboratory of Earth System Numerical Modeling and Application, University of Chinese Academy of Sciences, Beijing 101408, China
[f] Department of Geological Sciences, Stanford University, CA 94305, USA
[g] Department of Energy and Power Engineering, Tsinghua University, Beijing 100084, China
[h] Department of Petroleum Engineering, University of Houston, TX 77023, USA
[i] Eastern Institute for Advanced Study, Ningbo 315200, China

ARTICLE INFO

Article history:
Received 27 March 2025
Received in revised form 15 July 2025
Accepted 16 July 2025
Available online xxxx

Keywords:
CO_2 capture
Utilization, and storage
THMC coupling
Numerical models
Carbon-resilient world

ABSTRACT

Geological storage and utilization of CO_2 involve complex interactions among Thermo-hydro-mechanical-chemical (THMC) coupling processes, which significantly affect storage integrity and efficiency. To address the challenges in accurately simulating these coupled phenomena, this paper systematically reviews recent advances in the mathematical modeling and numerical solution of THMC coupling in CO_2 geological storage. The study focuses on the derivation and structure of governing and constitutive equations, the classification and comparative performance of fully coupled, iteratively coupled, and explicitly coupled solution methods, and the modeling of dynamic changes in porosity, permeability, and fracture evolution induced by multi-field interactions. Furthermore, the paper evaluates the capabilities, application scenarios, and limitations of major simulation platforms, including TOUGH, CMG-GEM, and COMSOL. By establishing a comparative framework integrating model formulations and solver strategies, this work clarifies the strengths and gaps of current approaches and contributes to the development of robust, scalable, and mechanism-oriented numerical models for long-term prediction of CO_2 behavior in geological formations.

Contents

* Corresponding authors.
E-mail addresses: jial@ucalgary.ca (L. Jiang), fushenliu@zju.edu.cn (F. Liu).

Please cite this article as: N. Zhang, L. Jiang, F. Liu et al., Advances in thermo-hydro-mechanical-chemical modelling for CO_2 geological storage and utilization, International Journal of Mining Science and Technology, https://doi.org/10.1016/j.ijmst.2025.07.010

1. Introduction

Global CO_2 emissions reached a record high of 36.8 Gt in 2022 [1], and the atmospheric concentration of CO_2 has dramatically surged over the past century due to substantial emissions. Its contribution to the greenhouse effect is now a scientific consensus. However, improving energy efficiency alone cannot fundamentally eliminate CO_2 emissions, and the large-scale application of renewable energy technologies faces challenges in the short term. Therefore, CO_2 capture, utilization, and storage (CCUS) represent the most direct and critical technological approach for reducing CO_2 emissions and achieving carbon neutrality goals, providing essential support for these objectives [2]. This technology encompasses key processes such as CO_2 capture, transportation, geological storage, and utilization. Geological storage and utilization are core components of CCUS technology, offering advantages of large storage volumes, long storage durations, and enhanced development of deep underground resources. These factors determine its development potential and direction, presenting an effective means for achieving carbon neutrality in the future. Numerous projects worldwide have entered the industrial demonstration or commercial application stage. CO_2 geological storage and utilization involve injecting captured CO_2 into geological formations through engineering technology, utilizing geological conditions to produce or enhance energy and resource extraction, and achieving the long-term or permanent isolation of CO_2 from the atmosphere [3].

As shown in Fig. 1, after CO_2 is injected into the geological formation, it leads to an increase in pore pressure in the injection area [4], causing changes in the effective stress field (process (1)). These changes in the stress field affect rock porosity, permeability, capillary pressure, and thermal conductivity, thereby influencing the injection and flow of CO_2 (process (2)), heat transfer processes (process (3)), as well as solute transport and chemical reactions (process (5)). Additionally, the temperature of the injected CO_2 differs from the ambient formation temperature, leading to changes in the temperature field in the injection area (process (7)) [5]. The alteration in the temperature field due to CO_2 injection and migration has two main effects: changing the density and viscosity of the fluid, which will feedback to the injection and migration of CO_2 (process (8)); directly affecting the stress state of the rock as a temperature load (process (4)). Given the large period of CO_2 geological storage, the chemical interactions among CO_2, formation fluid, and rocks cannot be overlooked. The CO_2-H_2O-rock interactions lead to the dissolution or precipitation of minerals in the rock, which changes the flow pathways of fluids and the physical properties of the rock. This indirectly affects the hydraulic field (process (9)) and stress field (process (6)); simultaneously, chemical reactions involve both endothermic and exothermic processes, and therefore, CO_2-H_2O-rock interactions also influence the temperature field (process (11)). Conversely, changes in the temperature field and hydraulic field also affect the rates and directions of chemical reactions [6], altering the processes of chemical reactions between CO_2, H_2O, and rocks (processes (12) and (10)). Thus, CO_2 geological storage and utilization is a complex, coupled multi-physics process involving Thermo-hydro-mechanical-chemical (THMC) interactions.

On the whole, the THMC changes induced by CO_2 injection into geological formations are complex and interrelated. The injection of CO_2 leads to temperature changes, causing a local decrease in temperature due to the absorption of heat during CO_2 expansion [7]. Hydraulically, CO_2 injection alters groundwater flow patterns, impacting pore pressure and fluid mobility through dissolution and diffusion processes. Mechanically, the injection can induce stress changes in the formation, leading to pore compression and potential deformation, which affects rock stability. Chemically, CO_2 reacts with minerals and groundwater, causing dissolution, precipitation, or the formation of new minerals, which alters the physical and chemical properties of the formation. These THMC

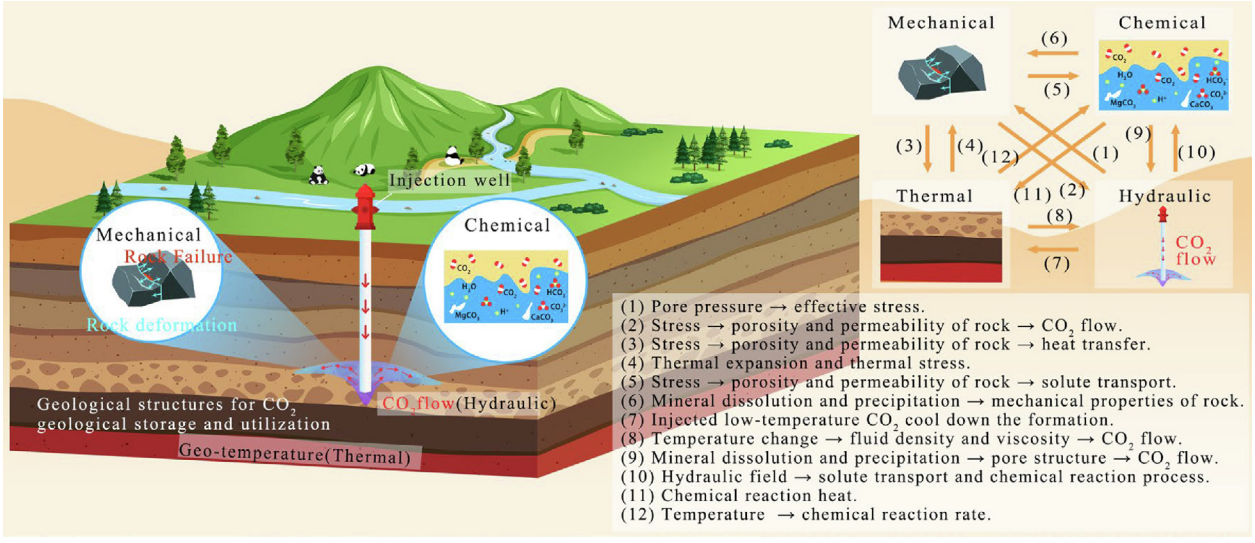

Fig. 1. The THMC coupling process in the CO_2 geological storage and utilization.

Table 1
Features of mainstream commercial software and open-source frameworks for THMC coupled simulations.

Software	Main feature	Advantage	Limitation	Application scenario	Additional feature
TOUGH series	Multiphase flow, THC coupling (ECO_2N module), chemical kinetics (TOUGH REACT), geomechanics (TOUGH-CSM)	Modular design offers flexibility; open-source; widely used in academia; optimized for saline aquifer CO_2 storage	Limited geomechanical coupling (requires plugins); low parallel efficiency; less intuitive interface	Lab- to field-scale studies (e.g., CO_2 migration, mineral reactions)	Includes specialized modules (ECO_2N, TMVOC); supports hydrate and unsaturated zone modeling
CMG-GEM	Full THMC coupling (multiphase flow, chemical equilibrium, geomechanics)	Mature commercial platform; user-friendly interface; dominant in CO_2-EOR projects; stable algorithms	High licensing costs; simplified chemical modules; limited customization	Engineering-scale CO_2-EOR simulations	Supports multi-resolution modeling (reservoir-wellbore); integrates geostatistical inversion tools
COMSOL multiphysics	Flexible THMC coupling with customizable equations	Intuitive GUI; ideal for small-scale mechanistic studies; dynamic multiphysics interaction	Low efficiency for large-scale simulations; requires external tools for engineering applications; expensive licenses	Pore-scale or lab-scale mechanism validation	Finite element-based; extensive predefined physics interfaces
OpenGeoSys (OGS)	Open-source THMC coupling (porous/fractured media); monolithic/staggered solvers	Free and open-source; supports cross-scale modeling (pore-reservoir); community-driven updates	Steep learning curve; limited parallel optimization; few engineering case studies	Geothermal, nuclear waste disposal, and long-term CO_2 storage studies	Enables equivalent constitutive parameter bridging; applied to concrete degradation and CO_2 storage
PHREEQC	Water-rock chemical reactions (static/dynamic equilibrium)	Comprehensive chemical database; integrates with flow simulators (e.g., TOUGH); ideal for lab-scale batch reactors	No multiphase flow capability; requires external frameworks for transport simulations; limited to chemical field coupling	Chemical mechanism analysis (e.g., mineral dissolution-precipitation)	Often coupled with TOUGH/OGS; supports IPHREEQC API extensions
AEEA coupler	Sequential THMC coupling via ABAQUS (geomechanics) and ECLIPSE (fluid flow)	Efficient cross-software integration; validated in Shenhua CCUS project; flexible parameter transfer.	Dependent on external software; time-step synchronization errors; limited to specific commercial tools.	Field-scale engineering (e.g., caprock stress analysis)	Developed by Institute of Rock and Soil Mechanics, Chinese Academy of Sciences; supports dynamic CO_2 front tracking
GEOSX	High-performance THMC coupling (multi-scale, parallel computing)	Billion-cell grid support; GPU acceleration; active open-source community.	Early development stage; limited real-world applications; incomplete documentation.	Large-scale reservoir simulations and long-term storage predictions	Developed by Lawrence Livermore National Lab; integrates ML-based uncertainty quantification

changes collectively influence the efficiency and safety of CO_2 storage.

Currently, commercial software and open-source frameworks for THMC multi-field coupled simulation of CO_2 geological sequestration and utilization exhibit a diversified landscape, yet these tools still face challenges in terms of functionality completeness and engineering applicability (Table 1). Tools such as the TOUGH series, CMG-GEM, and COMSOL each have their distinct features: the TOUGH series is widely used in academic research through its modular design (e.g., TOUGHREACT for coupled chemical kinetics and TOUGH-CSM for integrating mechanical fields), but its mechanical coupling capabilities are less advanced compared to the commercial software CMG-GEM, which holds an advantage in CO_2 enhanced oil recovery projects due to its mature THMC fully coupled algorithm; meanwhile, COMSOL is renowned for its flexible multi-physics coupling ability but is limited by computational efficiency, making it difficult to support large-scale reservoir simulations. Emerging technologies such as the AEEA Coupler from the Institute of Rock and Soil Mechanics, Chinese Academy of Sciences, which bridges ABAQUS and ECLIPSE to achieve cross-software collaboration, and the open-source framework GEOSX, which focuses on high-performance parallel computing and multi-scale modeling, also exist. However, most tools still exhibit significant shortcomings. On one hand, their fully coupled capabilities are insufficient—for example, PHREEQC requires external code to extend multiphase flow simulations, and the TOUGH series depends on plugins to supplement dynamic interactions of mechanical fields; On the other hand, engineering-scale applications are constrained by computational efficiency, with slow progress in parallel optimization for billion-grid cell models and GPU acceleration, and the lack of a unified framework for pore-core-reservoir cross-scale parameter transfer makes it challenging to balance the accuracy and cost of surrogate models. In practical terms, CMG-GEM has been successfully applied in projects such as the Weyburn-Midale CO_2-EOR operation, while TOUGH-REACT is commonly used in risk assessments prior to CO_2 injection. These examples reflect a broader trend: commercial simulators offer stronger integration and field readiness for large-scale deployment, whereas open-source tools provide valuable flexibility for mechanistic research and model prototyping.

THMC coupling processes are both a prerequisite for the efficient development of resources such as CO_2-enhanced oil/gas and geothermal energy and a necessary condition for the successful implementation of CO_2 storage. Simultaneously, under the THMC coupling conditions, the integrity of cap rocks may be damaged, resulting in CO_2 leakage. Therefore, THMC-coupled numerical simulations are a critical and core technology to ensure the safe and stable long-term storage of CO_2, optimize CO_2 injection parameters, and analyze the mechanisms of enhanced resource development with CO_2. Currently, scholars have conducted detailed reviews on the numerical simulation of THMC coupling in the process of CO_2 geological storage and utilization, discussing the existing problems and challenges in this area of research.

In recent years, scholars have published a number of review articles summarizing the progress and challenges of THMC numerical simulation in CO_2 geological storage and utilization. While these studies have substantially contributed to establishing a foundational understanding of THMC processes, they differ considerably in scope and analytical depth. Many reviews focus on physical or geochemical mechanisms—such as mineral reactions and thermal effects—or on simulator platforms and field-scale applications (Table 2), but often lack systematic assessment of the underlying mathematical models or numerical solution techniques. Others provide valuable technical summaries but offer limited evaluation of modeling assumptions, algorithmic performance, or computational limitations (Table 3). In particular, few studies explicitly address the integration of numerical algorithms with multi-scale geological heterogeneity, which is essential for robust THMC modeling.

Against this backdrop, this work provides a comprehensive review of research on the numerical simulation of THMC coupling in the process of CO_2 geological storage and utilization. It introduces the progress in research on the mathematical models of THMC coupling problems and numerical solutions for these coupling issues during the CO_2 geological storage process. This work also summarizes the main problems currently faced by numerical simulation technologies in CO_2 geological storage and utilization, aiming to offer references for research on CO_2 storage and utilization mechanisms, caprock stability prediction, and other aspects involved in the process of CO_2 geological storage and utilization.

2. THMC coupling governing equations

The research object of the multi-physics coupled numerical simulation for CO_2 geological storage and utilization involves a multiphase, multicomponent system composed of the solid rock skeleton and porous fluid [27]. The governing equations mainly include stress balance equations, hydraulic field equations, energy conservation equations, and chemical field equations [28].

Table 2
Overview of review articles on the multi-field coupling in CO_2 geologic storage and utilization.

Reference	Year	Main content	Proposed directions for further research
Yu et al. [8]	2023	Governing equations, numerical solutions, application examples	Numerical algorithms, governing equations, parallel solving algorithms
Cheng et al. [9]	2023	Earthquake-inducing conditions, simulators	Field application of mathematical models, field data acquisition
Eyinla et al. [10]	2023	Thermal stress, effect of CO_2 injection rate and volume, porosity changes under CO_2, changes in rock properties	Monitoring during sequestration
Wu et al. [11]	2020	Chemical reaction mechanisms, heat transfer processes, storage potentials	CO_2-H_2O-rock reaction, mineral dissolution, precipitation, temperature effects on dissolution
Temitope et al. [12]	2019	Physical processes, governing equations	Multi-scale simulation, CO_2 leakage monitoring
Akono et al. [13]	2019	Chemical reaction processes, reaction kinetic parameters, reservoir physical changes under thmc coupling condition, simulators	Fluid-pore interaction, chemical reaction, mechanical behavior, multiscale modeling
Masoudian [14]	2016	Physical processes, multiphase-multiscale flow, rock deformation, adsorption-induced deformation	Rock microstructure, adsorption mechanism, geomechanical characteristics, mathematical modeling
Abidoye et al. [15]	2015	Storage mechanism, two-phase flow, physical parameter changes under the action of CO_2, CO_2 leakage, and monitoring	CO_2 storage in different rock types, chamber experiments, two-phase flow patterns
Song et al. [16]	2013	Permeability evolution, CO_2 leakage pathways, simulators	Governing equations, experimental tests, multiphase flow modeling
Jiang [17]	2011	Governing equations, simulators	Large-scale field modeling, solution algorithms

Table 3
Overview of review articles on simulating THMC coupling processes.

Reference	Year	Field of research	Main content
Zhang et al. [18]	2023	Geothermal development, oil and gas development, CO_2 storage	Governing equations, solution methods
Liu et al. [19]	2023	Geothermal development	Physical processes, indoor experiments, commercial software, open-source simulators
Khandoozi et al. [20]	2023	CO_2 storage	Physical processes, storage mechanisms, simulators
Li et al. [21]	2022	Geothermal development	Governing equations, numerical simulation cases
Birkholzer et al. [22]	2019	Nuclear waste disposal	Physical processes, field experiments, indoor experiments
Pandey et al. [23]	2018	Geothermal development	Mathematical modeling, solution methods
Wang et al. [24]	2017	Shale and tight gas development	Physical processes, governing equations, simulators
Li et al. [25]	2013	CO_2 Saline storage	Mathematical modeling, solution methods
Rutqvist et al. [26]	2012	Geomechanics	Field experiments, indoor experiments

2.1. The stress balance equations

The fully coupled THMC model for CO_2 geological storage and utilization integrates theories of porous elasticity, thermoelasticity, elastoplasticity, and reactive solute transport to handle the strong coupling effects between heat flux, reactive solute transport, fluid flow [29], and deformation of porous media. Based on the thermo-poroelasticity theory of single-phase fluid flow in deformable porous media, the general equilibrium equation with effective stress as a variable can be expressed as [30]:

$$G\nabla^2\mathbf{u} + (G+\lambda)\nabla \mathrm{div}\mathbf{u} - \left(1-\frac{K}{K_\mathrm{m}}\right)\nabla p - K\beta_\mathrm{s}\nabla T = 0 \tag{1}$$

where G and λ are Lamé elastic constant; $\mathbf{u}$, p and T the displacement, pore pressure, and temperature, respectively; β_s the volume thermal expansion coefficient of the rock skeleton; K and K_m the bulk modulus of the porous media and solid matrix, respectively.

Eq. (1) is generally applicable to homogeneous formations. However, for reservoirs containing natural fractures [29], it is necessary to consider the influence of these fractures, as well as the stress variations caused by gas adsorption and desorption in porous media. Taking a fractured coal rock as an example, which is a typical dual-porosity material, its mechanical properties are significantly influenced by internal pores and fractures. Considering the expansion caused by thermal stress, effective stress induced by fluid pressure in the matrix and fractures, and expansion/contraction caused by gas adsorption/desorption, the total strain of the coal can be defined as [31]:

$$G_\mathrm{s}u_{k,ll} + \frac{G_\mathrm{s}}{1-2\upsilon}u_{l,lk} - (\alpha_\mathrm{m}p_{\mathrm{m},k} + \alpha_\mathrm{f}p_{\mathrm{f},k}) - K_\mathrm{V}\alpha_\mathrm{T}T_{,k} - K_\mathrm{V}\left(\sum_{i=1}^{2}\frac{\varepsilon_{\mathrm{L},\,i}b_i p_{\mathrm{mg},\,i}}{1+\sum_{j=1}^{2}b_j p_{\mathrm{mg},j}}\right) + f_k = 0 \tag{2}$$

where G_s is the shear modulus; u the displacement; υ the Poisson's ratio; α_m the Biot effective stress coefficient for coal matrix; α_f the Biot effective stress coefficient for fractures; p_m the fluid pressure in the coal matrix; p_f the fluid pressure in fractures; K_V the bulk modulus; α_T the thermal expansion coefficient; T the temperature of the coal; $\varepsilon_{\mathrm{L},i}$ the Langmuir-type strain coefficient, which represents the maximum swelling capacity; b the fracture aperture; $p_{\mathrm{mg},i}$ the gas pressure of component i in the matrix, i=1 corresponds to methane, and$i$ = 2 corresponds to CO_2; and f_k the coal gravity.

In Eq. (2), the first and second terms represent the influence of ground stress, with the second term indicating the effect of fluid pressure in the matrix and fractures. The third term represents thermal stress, the fourth term represents stress induced by gas adsorption/desorption, and the fifth term represents the influence of gravity.

2.2. The hydraulic field equations

After CO_2 injection, a mixed fluid is formed with the formation water. The fluid flow facilitates the transport and exchange of substances within the system [32]. Reactivity occurs between CO_2 and the formation water, leading to localized chemical reactions with minerals. Considering single-phase fluid flow within the reservoir and incorporating Darcy's law, the general form of the fluid flow continuity equation can be expressed as [33]:

$$\nabla^T\left(-\frac{k}{\mu}\nabla p\right) + \left(\frac{\alpha-\phi}{K_\mathrm{m}} + \frac{\phi}{K_\mathrm{w}}\right)\frac{\partial p}{\partial t} + \alpha\frac{\partial \varepsilon}{\partial t} - [(\alpha-\phi)\beta_\mathrm{s} + \phi\beta_\mathrm{w}]\frac{\partial T}{\partial t} = 0 \tag{3}$$

where k is the rock permeability; μ the fluid viscosity; p the fluid pressure; α the Biot coefficient; ϕ the porosity; K_w the fluid bulk modulus within the pores; ε the strain; β_s the volumetric coefficient of thermal expansion of the skeleton; β_w the volumetric coefficient of thermal expansion of the fluid; and t the time.

In fact, after CO_2 injection into the formation, it will not be completely miscible with the formation water but will form a two-phase flow with it. The single-phase Darcy flow represented in Eq. (3) is a simplification of the actual situation in the formation and does not adequately describe the fluid flow process within it. To better characterize the multiphase fluid seepage in the formation, the multiphase fluid seepage equation must be established [34]:

$$\frac{\partial \phi S_\mathrm{lp}\rho_\mathrm{lp}}{\partial t} + \nabla\cdot\left[-\frac{\rho_\mathrm{lp}kk_\mathrm{rlp}}{\mu_\mathrm{lp}}\left(\nabla p_\mathrm{lp} + \rho_\mathrm{lp}g\nabla z\right)\right] = R_\mathrm{lp} \tag{4}$$

where the subscripts lp denote the phase, c for CO_2, w for water and o for oil; S_c the saturation of the phase lp; ρ_lp the density of the phase lp; k_rlp the relative permeability of the phase lp; μ_lp the viscosity of the phase lp; p_lp the pressure of the phase lp; z the stratigraphic depth; and R_lp the source-sink term of the phase lp, which can represent the production and consumption of material as a result of chemical reactions.

Both Eqs. (3) and (4) characterize single-phase or two-phase fluid seepage within the matrix. However, most reservoirs contain natural fractures, and the two-phase fluid flow of gas and water within these fractures must be considered. In such cases, CO_2 and formation water coexist in the fracture-matrix system, and the gas–water mixture is transported in a two-phase flow within the matrix and fractures. The equation of mass conservation can be expressed as [31]:

$$\begin{cases} \underbrace{\frac{\partial\left(s_\mathrm{g}\phi_\mathrm{f}\rho_{\mathrm{fg},i}\right)}{\partial t} + \nabla\cdot\left(\rho_{\mathrm{fg},i}q_{\mathrm{g},i}\right)}_{\text{Gas phase in fracture}} + \underbrace{\frac{\partial\left(s_\mathrm{w}\phi_\mathrm{f}\rho_{\mathrm{fgd},i}\right)}{\partial t} + \nabla\cdot\left(\rho_{\mathrm{fgd},i}q_\mathrm{w}\right)}_{\text{Dissolved gas in water phase in fracture}} = \underbrace{\frac{1}{\tau_i}\frac{M_{\mathrm{g},i}}{RT}\left(p_{\mathrm{mg},i} - p_{\mathrm{fg},i}\right)}_{\text{Gas from (or to) matrix}} \\ \underbrace{\frac{\partial(s_\mathrm{w}\phi_\mathrm{f}\rho_\mathrm{w})}{\partial t} + \nabla\cdot(\rho_\mathrm{w}q_\mathrm{w})}_{\text{Water phase in fracture}} + \underbrace{\frac{\partial\left(s_\mathrm{g}\phi_\mathrm{f}\rho_\mathrm{fv}\right)}{\partial t} + \nabla\cdot\left(\rho_\mathrm{fv}\sum_{i=1}^{2}q_{\mathrm{g},i}\right)}_{\text{Water vapour in gas phase in fracture}} = 0 \end{cases} \tag{5}$$

where s_g is the gas saturation; ϕ_f the equivalent porosity of the fracture; $\rho_{\mathrm{fg},i}$ the density of the components i in the fracture; $q_{\mathrm{g},i}$ the velocity of the components i in the fracture; s_w the water sat-

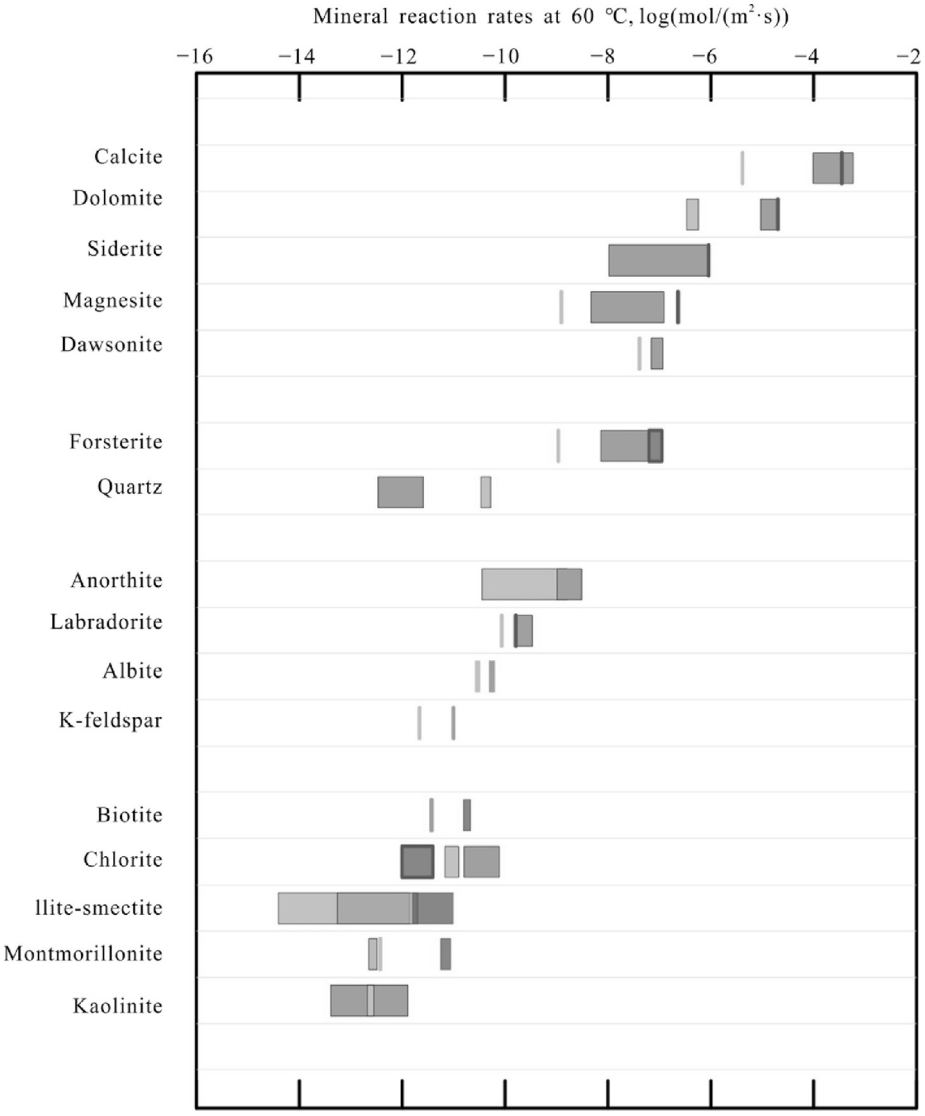

Fig. 2. Summary of mineral reaction rates at 60 °C [39].

uration; $\rho_{fgd,i}$ the density of the dissolved gas; q_w the velocity of the aqueous phase; τ_i the desorption time of the gas components i; $M_{g,\,i}$ the molar mass of the gas components i; R the gas constant; $p_{fg,i}$ the gas pressure of the components i in the fracture; ρ_w the density of water; and ρ_{fv} the density of the saturated vapor.

The CO_2 adsorption process in coal rocks is usually described by the Langmuir model [35]:

$$V_{ep} = \frac{a_{mac} b_{cp} p_{ep}}{1 + b_{cp} p_{ep}} \tag{6}$$

where V_{ep} is the adsorption capacity at equilibrium pressure; a_{mac} the maximum adsorption capacity of the coal sample; b_{cp} the comprehensive parameters of adsorption, desorption speed, and adsorption heat; and p_{ep} the equilibrium pressure of CO_2.

For shale, the desorption process is irreversible and a desorption model is required [36]:

$$V_{des} = \frac{V_d p_g}{p_d + p_g} + c_r \tag{7}$$

where V_{des} is the desorption amount of shale; V_d the maximum adsorption capacity of shale sample during desorption; p_d the comprehensive function of adsorption rate, desorption rate and adsorption heat; c_r the residual adsorption capacity under deficient pressure; and p_g the gas pressure.

2.3. The energy conservation equations

Assuming energy is solely a function of temperature, and that heat flux within the porous media is generated only through thermal convection and thermal conduction [37], the derived energy conservation equation is [38]:

$$\frac{dU_i}{dt} = \nabla \cdot F_i + q_i \tag{8}$$

where U_i is the heat accumulation term for rocks and fluids; F the heat transfer term; and q_i the source/sink term resulting from heat injection or extraction.

For component i, the heat accumulation term is given by:

$$U_i = (1-\phi)\rho_R C_R T + \phi \sum_\beta S_\beta \rho_\beta u_\beta^i \tag{9}$$

where ρ_R is the rock density; C_R the specific heat capacity of the rock; the subscript β the phase (CO_2 or water); S the saturation; ρ the density; and u the specific internal energy.

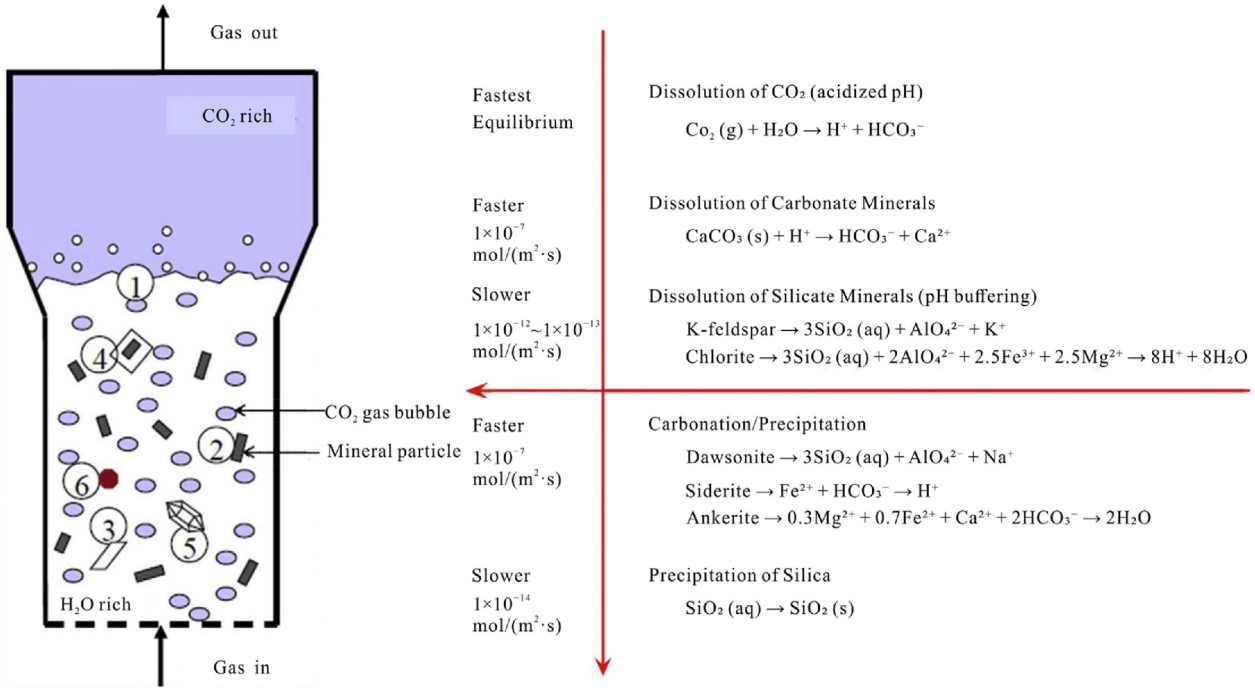

Fig. 3. The chemical reaction process between CO_2 and rock minerals [40].

Ignoring radiative heat transfer, the heat flux is composed of the terms for thermal conduction and thermal convection, and its expression is given by:

$$F_i = -\kappa\nabla T + \sum_{\beta}\rho_{\beta}h_{\beta}^{i}\left[-\frac{kk_{\mathrm{r}}^{i}}{\mu_{\beta}}\cdot\left(\nabla P_{\beta}-\rho_{\beta}g\nabla z\right)\right] \tag{10}$$

where κ is the thermal conductivity; h the specific enthalpy; μ the viscosity; and k_r the relative permeability.

2.4. The chemical field equations

The chemical reactions between CO_2 and rock minerals are highly complex, influenced mainly by factors such as rock type, composition, and temperature (Fig. 2), pH=8 under low-CO_2 (light grey bars), pH=4 under low-CO_2 (grey bars), and pH=4 under elevated-CO_2 conditions (dark grey bars) in the figure. As depicted in Fig. 3, upon the entry of CO_2 into the reservoir, the dissolution of CO_2 is the most rapid chemical reaction, achieving equilibrium immediately after injection while simultaneously releasing a large quantity of H^+. Subsequent reactions of carbonate minerals like calcite, dolomite, and magnesite with H^+ occur at rates of the order of 10^{-7} mol/(m^2·s), quickly reaching equilibrium. In contrast, silicate minerals such as the feldspar group, kaolinite group, illite group, montmorillonite group, and chlorite group, react with H^+ more slowly, with rates varying from 10^{-13} to 10^{-12} mol/(m^2·s); these reactions may take millennia to show significant effects. Besides dissolution processes, the formation and precipitation of new, mainly stable carbonate minerals such as magnesite, siderite, and ankerite occur at faster rates, approximately 10^{-7} mol/(m^2·s). The slowest reaction is quartz precipitation, at a rate of 10^{-14} mol/(m^2·s). The latter two processes constitute the primary mechanisms of CO_2 mineral sequestration.

For the complex chemical reactions involving CO_2, H_2O, and rock minerals described above, the chemical reaction source-sink term is used to represent these processes in the hydraulic field equation (Eq. (4)) and can be integrated into Eq. (5). Its expression is:

$$R_{\mathrm{lp}} = -\xi\cdot r \tag{11}$$

where ξ is the stoichiometric coefficient for chemical reactions; and r the chemical reaction rate for mineral dissolution and mineralization reactions.

The expression for the chemical reaction rate r is [40]:

$$r = \pm K_n A_n\left|1-\Omega_n^{\theta}\right|^{\eta}(n=1,\ldots,N_{\mathrm{q}}) \tag{12}$$

where K_n is the temperature-dependent rate constant; A_n the specific reaction surface area; Ω_n the saturation ratio of kinetic minerals; and θ and η the usually taken as 1.

In Eq. (12), a positive value of r corresponds to mineral dissolution, whereas a negative value indicates precipitation.

Considering multiple reaction mechanisms, mineral dissolution and precipitation are not only influenced by pure H_2O (at neutral pH) but also catalyzed by H^+ and OH^-. Thus, the equation for the rate constant K_n comprises three terms:

$$K_n = k_{25}^{n}\exp\left[\frac{-E_a^n}{R}\left(\frac{1}{T}-\frac{1}{298.15}\right)\right]+k_{25}^{H^+}\exp\left[\frac{-E_a^{H^+}}{R}\left(\frac{1}{T}-\frac{1}{298.15}\right)\right]a_{H^+}^{n_{H^+}} + k_{25}^{OH^-}\exp\left[\frac{-E_a^{OH^-}}{R}\left(\frac{1}{T}-\frac{1}{298.15}\right)\right]a_{OH^-}^{n_{OH^-}} \tag{13}$$

where k_{25} is the rate constant at 25 °C; E_a the activation energy; and $a_{H^+}^{n_{H^+}}$ and $a_{OH^-}^{n_{OH^-}}$ the activities of H^+ and OH^-, respectively.

The representation of ionic concentration changes in chemical reaction processes necessitates selecting a set of independent primary species from which all other species (including minerals) can be derived. Chemical substances that can be expressed as combinations of primary species are termed secondary species. The mass conservation equation for the chemical reaction process, expressed in terms of the total molar concentration j of the primary species Ψ_j is [41]:

$$\frac{\partial}{\partial t}(\phi\Psi_j)+\nabla\cdot(\boldsymbol{q}-\phi D\nabla)\Psi_j+\sum_{m=1}^{N_m}\upsilon_{jm}I_m-q_j=0,\quad j=1,2,\ldots,N_c \tag{14}$$

Table 4
The characteristics of different constitutive relationship models.

Constitutive model type	Assumption	Advantage	Disadvantage	Typical mathematical expression
Elastic constitutive model	Assumes rocks exhibit behavior within the 'small strain' range	Easy convergence of calculation results; highly feasible for coupled multi-field calculations	Unable to consider the plastic deformation of rocks over long timescales and under complex stress conditions	$\sigma = E\varepsilon$ [44]
Plastic constitutive model	Assumes a nonlinear relationship between stress and strain	Describes the nonlinear behavior of rocks under large stress or strain effectively	The complexity of the model leads to higher computational costs	$\dot{\boldsymbol{\sigma}} = \boldsymbol{C}_{ev} : (\dot{\varepsilon} - \dot{\varepsilon}_p)$ [45]
Thermo-elastic/plastic constitutive model	The thermal expansion or contraction of rocks is coupled with their elastic response	Reflects the relationship between temperature and stress	Involves a large computational workload	$\sigma_{ij} = D_{ijkl}\varepsilon_{kl} - \alpha'_{ij}p + \chi_{ij}\Delta C^S - \Lambda_{ij}\Delta T$ [46]
Mechanical damage constitutive model	Rocks accumulate damage during the loading process, leading to changes in their mechanical properties	Capable of characterizing the failure modes of rocks under different loading conditions	Large computational cost and difficulty in determining mechanical damage parameters	$\sigma = E_n \cdot \left(\exp\left(-\left(\frac{\varepsilon}{\lambda}\right)^m\right)\right) \cdot \varepsilon$ [47]
Chemical damage constitutive model	Chemical reactions, such as mineral dissolution and precipitation, alter the microstructure and macroscopic mechanical properties of rocks	Reflects changes in the mechanical properties of rocks under the chemical action of CO_2	Large computational cost and difficulty in determining chemical damage parameters	$\sigma = \tilde{\sigma}(1-D) = E\varepsilon(1-D)$ [48]

where Ψ_j is the total molar concentration of the primary species j; $\boldsymbol{q}$ the Darcy flux; N_m the number of minerals formed by the kinetic reaction; υ_{jm} the stoichiometric coefficient of the primary species j in the m th kinetic reaction; I_m the reaction rate of the m th mineral; and q_j the source-sink phase of the primary species j.

The total molar concentration of the primary species can be expressed as [42]:

$$\Psi_j = C_j + \sum_{i=1}^{N_s} \upsilon_{ji} C_i \tag{15}$$

where C_j is the concentration of the primary species; C_i the concentration of the i th secondary species; N_s the number of the secondary species; and υ_{ji} the stoichiometric coefficients.

The physicochemical interactions between CO_2-H_2O and formation rocks can also lead to changes in the porosity and permeability of formation rocks. The porosity related to rock minerals φ_c is:

$$\varphi_c = 1 - \sum_{m=1}^{N_m} f_m - f_u \tag{16}$$

where φ_c is the porosity related to the minerals; N_m the total number of reactive minerals; and f_m and f_u the volume fractions of reactive and nonreactive minerals, respectively.

Therefore, the porosity evolution model considering mechanical deformation and chemical reactions can be written as:

$$\varphi = \varphi_m + \Delta\varphi_c \tag{17}$$

where $\Delta\varphi_c$ is the porosity change induced by mineral precipitation and dissolution; and φ_m the porosity related to initial porosity and mechanical deformation.

The permeability evolution model related to the porosity and damage variable is:

$$k = k_0 \left(\frac{\varphi}{\varphi_0}\right)^3 \exp(\alpha_k D) \tag{18}$$

where k_0 is the initial absolute permeability; α_k the damage-permeability correlation coefficient, which takes a value of 5; and D the damage variable.

2.5. The Stress–strain constitutive models

The constitutive models used for the coupled simulation of THMC processes in CO_2 geological storage primarily encompass elastic constitutive model, plastic constitutive model, thermo-elastic/plastic constitutive model, mechanical damage constitutive model and chemical damage constitutive model (Table 4). Before 2006, the field of rock mechanics related to CO_2 geological storage saw relatively few research achievements. However, subsequent results have exhibited explosive growth, signifying escalating concern for the mechanical issues associated with CO_2 geological storage [43]. The evolution of constitutive models utilized in the coupled simulation of CO_2 storage has been marked by advancement from simple to complex, starting with elastic models and progressing to plastic and discontinuous models. There is also a trend towards accommodating the high-temperature, high-stress conditions typical of CO_2 storage environments, as well as the thermoelastic, thermoplastic, and damage constitutive models that consider the geochemical reactions resulting from CO_2-H_2O-rock interactions.

The elastic constitutive model is based on Hooke's law, assuming that rocks exhibit linear elastic behavior in the small-strain range and cannot consider the plastic deformation of rocks over a long time scale or under complex stress conditions. However, these constitutive models yield convergent results and are easy to perform highly coupled multi-physics simulations. Therefore, they still account for a considerable proportion of the multi-physics coupled simulations of CO_2 geological storage.

The plastic constitutive model mainly include elastoplastic constitutive model and viscoplastic constitutive model. This type of model considers the occurrence of plastic deformation in rocks when the stress exceeds a certain threshold, allowing for the

Table 5
Characteristics of coupling solution methods.

Method of Coupling	Characteristic	Advantage	Disadvantage	Applicability
Fully coupled method [49]	All governing equations are solved simultaneously at every time step	High accuracy	Computationally intensive; suitable only for small-scale, simple geometric models	Suitable for small-scale studies such as pore-scale or lab-scale mechanisms, e.g., mineral dissolution kinetics or fracture initiation under controlled conditions
Iterative coupled method [50]	Multiple iterations of the computation are performed within each time step until the convergence condition is satisfied	Higher computational efficiency	Poor computational convergence and long computational time in strongly coupled problems	Widely used in engineering-scale CCUS applications, such as CO_2-EOR and saline aquifer storage, where fluid–structure interaction is moderate and needs to be resolved iteratively
Explicit coupled method [51]	Within one time step, the computed results of some fields are unidirectionally transferred as external loads to other fields	High computational efficiency; good convergence; applicable to complex geometric models and complex intrinsic models	Lower computational accuracy	Increasingly applied in large-scale or long-term storage simulations, including fault slip prediction, caprock integrity assessment, and geothermal CO_2 applications

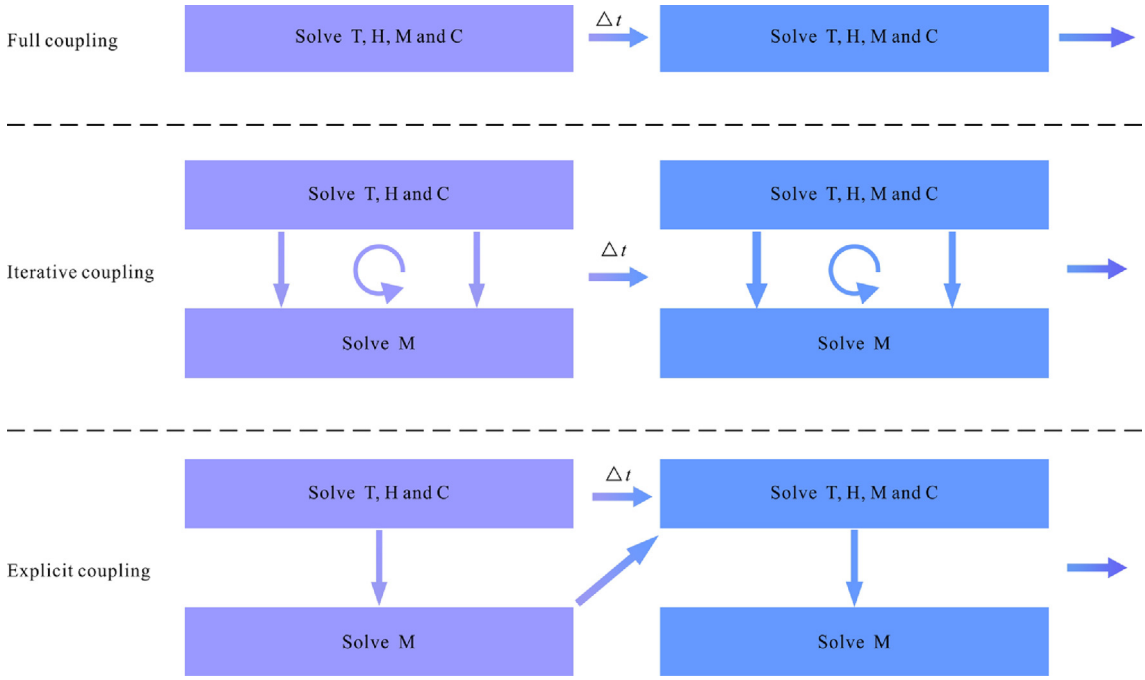

Fig. 4. Data transfer methods and solution routes for different coupling methods (modified after Yu et al. [8]).

description of nonlinear behavior in rocks under high-strain conditions. Under complex stress conditions, the mechanical response of reservoir and caprock formations does not obey the elasticity relation curve. Therefore, it is better to choose an elastoplastic constitutive model to characterize the deformation and yielding process. Especially when simulating the long-term creep characteristics of reservoir and caprock formations, a viscoplastic constitutive model should be used.

In addition, to reveal the influence of temperature and chemical damage on the stress–strain relationship during the CO_2 storage process, researchers have also developed thermo-elastic constitutive models, thermo-plastic constitutive model, chemical damage constitutive model, and mechanical damage constitutive model.

3. Methodologies for solving the governing equations

3.1. Coupling methods for the governing equations

Research on the multi-physics coupling process of CO_2 geological storage started relatively late. By drawing on coupling methods used in other engineering problems, such as the development of oil and gas resources, deep geothermal energy, and coal resources, methods suitable for solving the multi-physics coupling problems of CO_2 geological storage have been developed. These coupling solution methods mainly include fully coupled method, iterative coupling method, and explicit coupling method (Table 5).

The fully coupled method solves all the governing equations simultaneously. In this approach, all field variables are updated simultaneously after each iteration and are directly substituted into the overall stiffness matrix for the calculation of the next iteration step (Fig. 4). This method provides the highest degree of coupling and computational accuracy but requires significant computational effort and often takes a longer time to meet convergence requirements. It is suitable for small-scale studies, such as pore-scale or laboratory-scale mechanisms (e.g., mineral dissolution kinetics or fracture initiation under controlled conditions). Consequently, it is mostly applied to models with simple geometries and limited spatial scales, typically using elastic or plastic constitutive models.

The iterative coupled method performs multiple iterations within each time step. During each iteration step, the hydraulic field, energy conservation, and chemical reaction equations are first solved. The computed pore pressure is then transferred to the stress equilibrium equation to solve for rock deformation. Subsequently, rock properties such as porosity and permeability are updated based on the deformation. The process is repeated until convergence conditions are met before moving to the next time step (Fig. 4). Compared to the fully coupled method, the iterative coupled method significantly improves computational efficiency. It is widely used in engineering-scale CCUS applications, such as CO_2-EOR and saline aquifer storage, where fluid–structure interactions are moderate and best handled through iterative resolution.

In the explicit coupled method, equations for the hydraulic field, energy conservation, chemical reaction, and stress equilibrium are solved independently. Only the outputs, such as pore pressure, temperature, and saturation, from the current time step, serve as external loads for the stress equilibrium equation to update rock properties. However, the stress field calculation results do not feed into the flow or energy conservation equations within the same time step (Fig. 4). This method, with its lower degree of coupling and slightly reduced computational accuracy, offers high computational efficiency and good convergence. It is suitable for large-scale simulations under complex geological conditions and with complex rock constitutive models. This method is increasingly applied in large-scale or long-term CO_2 storage simulations, including fault slip prediction, caprock integrity assessment, and geothermal applications.

Although iterative and explicit coupling strategies offer a practical balance between computational tractability and coupling accuracy, their application to field-scale CO_2 geological storage scenarios often requires significant computational resources, particularly when dealing with fine spatial discretization, multi-physics interactions, and long simulation durations. In this regard, recent advances in High-performance computing (HPC) have provided critical computational support for the efficient execution of THMC simulations at large scales. HPC-enabled frameworks facilitate the parallelization of governing equation solvers and leverage GPU acceleration to enhance the convergence performance of iterative algorithms and reduce overall computation time. Notable examples include GEOSX, developed by Lawrence Livermore National Laboratory, which supports fully coupled THMC simulations across billion-cell reservoir models using distributed-memory architectures, and TOUGH3, which incorporates MPI-based parallelization to scale iterative multi-physics solvers. The integration of HPC technologies with coupling methods thus represents a key technical pathway for enabling high-fidelity, large-scale simulation of CO_2 injection, migration, and storage performance.

3.2. Numerical solution methods for governing equations

After constructing the THMC coupling mathematical model for CO_2 geological storage and utilization, it becomes necessary to employ specific numerical solution methods to discretize the governing equations and carry out numerical simulations. Currently, the commonly used numerical solution methods fall into three categories [18,52]: continuum methods, discrete methods, and quasi-continuous methods. Continuum methods include the finite volume method (FVM), finite element method (FEM), extended finite element method (XFEM), and the phase field method (PFM). Discrete methods mainly consist of the discrete element method (DEM), numerical manifold method (NMM), virtual internal bond model (VIB), and discretized virtual internal bonds (DVIB).

It is not straightforward to assert that one method is superior to others. Each method has its characteristics and presents advantages and disadvantages in computational effort, result accuracy, convergence, the difficulty of multi-field coupling, and ease of use (Table 6). Selecting the appropriate numerical solution method is critical and should consider the research objectives, influencing factors, and the morphology and dimensions of the geometric model for CO_2 geological storage and utilization.

Beyond the classification of numerical methods based on discretization principles, it is also essential to consider the modeling scale when analyzing THMC simulations in CCUS. At the microscopic scale, particularly within the pore and grain level, techniques such as the Lattice Boltzmann Method (LBM) and pore network modeling (PNM) have been extensively utilized to investigate multi-phase flow behavior, reactive transport, and interfacial phenomena. These methods are fundamentally different from macroscale approaches in their governing assumptions, resolution capacity, and computational structure. They enable detailed exploration of local mechanisms, such as capillary trapping and mineral alteration, which are often homogenized or parameterized in continuum-scale models. As such, incorporating scale-dependent modeling perspectives is critical for developing robust multi-scale simulation frameworks in CCUS.

4. Application of multi-physics coupled analysis

By employing multi-physics numerical simulations to calculate energy conservation, hydraulic field, stress field, and chemical field during and after the CO_2 injection process, one can analyze the

Table 6
Comparison of different numerical methods.

Numeric method type		Numerical method	Medium heterogeneity	Difficulty in Multi-Field Coupling	Calculation workload
Continuum medium method	Finite element model type	FEM	Y	*	***
		CZM	Y	*	**
		PFM	Y	*	***
		XFEM	Y	*	***
	Finite Volume Method	FVM	Y	*	**
	Boundary element method	DDM	N	***	*
	Mesh-free method	MFM	Y	*	****
Discrete medium method		DEM	Y	**	***
		Lattice model	Y	**	***
		NMM and DDA	Y	***	**
Quasi-continuum medium method		VIB and DVIB	Y	**	**

Notes: 1. In the "Medium heterogeneity" column, "Y" means that the heterogeneity of the medium can be characterized, "N" means that the heterogeneity of the medium cannot be characterized;
2. The more "*" in the column of "multi-field coupling", the greater the difficulty of multi-field coupling;
3. The more "*" in the "Calculation workload" column, the greater the calculation workload.

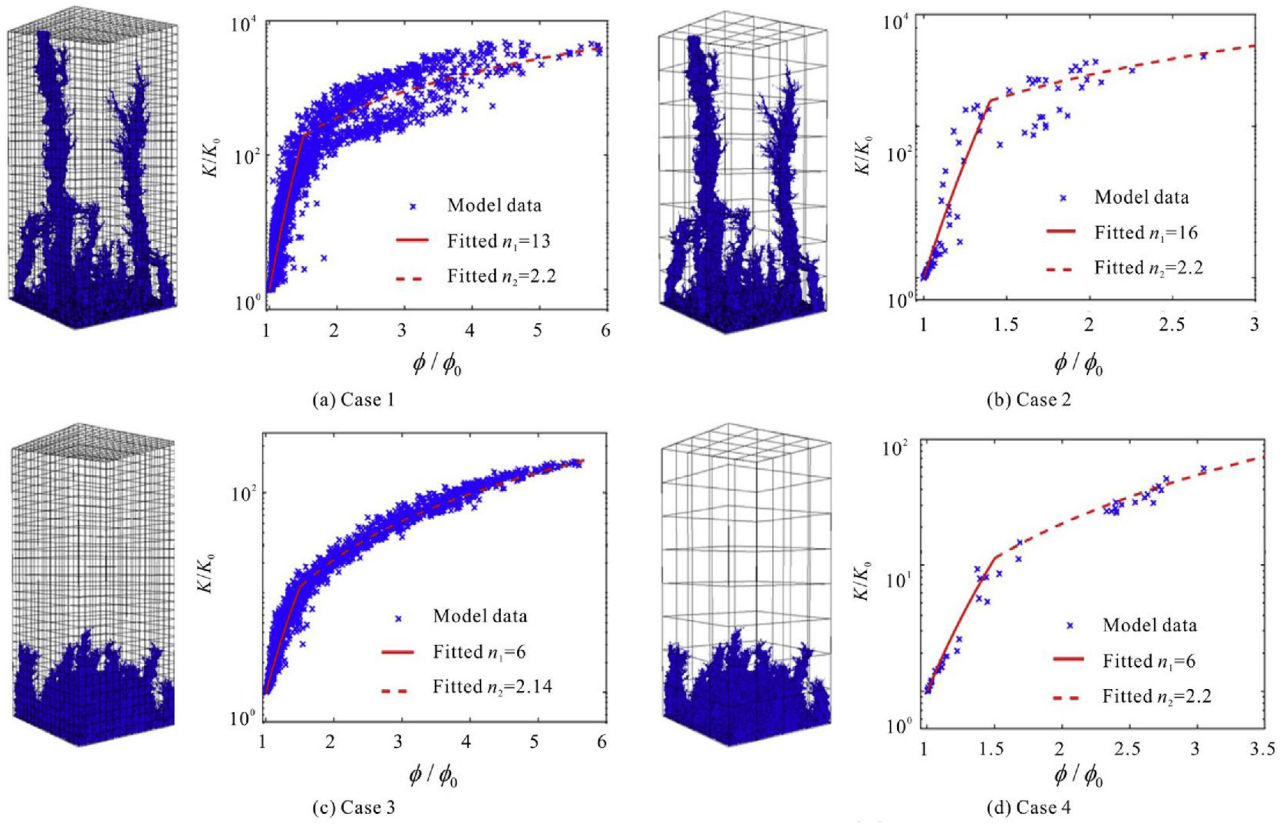

Fig. 5. The permeability variation caused by CO_2 alteration [54].

multiphase flow behavior of CO_2 and formation fluids, the CO_2-H_2O-rock chemical reaction process, as well as reservoir and caprock deformation and failure patterns. These analyses also aid in understanding the mechanical conditions that lead to the activation of natural fractures and faults. This section introduces the application of THMC coupling analysis in CO_2 geological storage and utilization, with a focus on studies related to storage mechanisms and quantities, caprock integrity assessment, surface deformation simulation, CO_2 fracturing simulation and CO_2 induced earthquakes.

4.1. Mechanisms and quantities of storage

The mechanisms of CO_2 storage include structural trapping, hydrodynamic trapping, residual trapping, mineral trapping, dissolution trapping, and adsorption trapping. Structural trapping is particularly focused on studying the structural integrity of the caprock using THMC coupling, considering the activation of natural fractures and faults due to mechanical effects. For other storage mechanisms, THMC coupling simulations are utilized to investigate CO_2 migration patterns, the dynamics of chemical reactions [53], the evolution of porosity and permeability due to chemical reactions (Fig. 5) [54], and the CO_2 adsorption capacity [55]. Through these studies, the quantities of CO_2 storage under different trapping mechanisms can be quantified [56].

4.2. Assessment of caprock integrity

The assessment of the mechanical integrity of caprock in the context of CO_2 geological storage and utilization using the THMC coupling method primarily involves two aspects: the risk of tensile failure in the reservoir and caprock caused by local high pressure due to injection pressure perturbation; and the risk of shear failure induced by local stress concentration under complex geological environments and changes in rock properties [57]. Specifically, the THM and THMC coupling models are currently used to study the stress field and the characteristics of its dynamic evolution in the storage system. Simulating the initial stress field and pressure perturbation caused by CO_2 injection (Fig. 6), alongside appropriate failure criteria and damage indicators, can reveal the mechanical conditions for different failure modes. The analysis takes into account factors such as temperature, time, injection rate, injection volume, and capillary forces, and their effects on the integrity of the caprock [58].

Furthermore, as formations often contain faults and natural fractures, the evolution of pore pressure directly impacts the geomechanical stability of these faults and fractures, which in turn may compromise the integrity of the caprock. Consequently, scholars use multiphase flow-geomechanics coupling methods to investigate the effects of injected CO_2 on the activation of faults (Fig. 7) [60] and natural fractures [61].

4.3. Surface uplift simulation

After CO_2 is injected into a reservoir, there is an increase in pore pressure and a corresponding decrease in skeleton stress within the injected area, leading to the expansion of pore volume. Additionally, CO_2 accumulation beneath the caprock exerts an upward force on the overlying strata. These two factors together cause the caprock to bend upward, resulting in surface deformation (Fig. 8).

Research on the multi-field coupling of surface deformation primarily focuses on the following aspects: (1) Utilizing a coupled fluid flow and geomechanics model to conduct numerical simula-

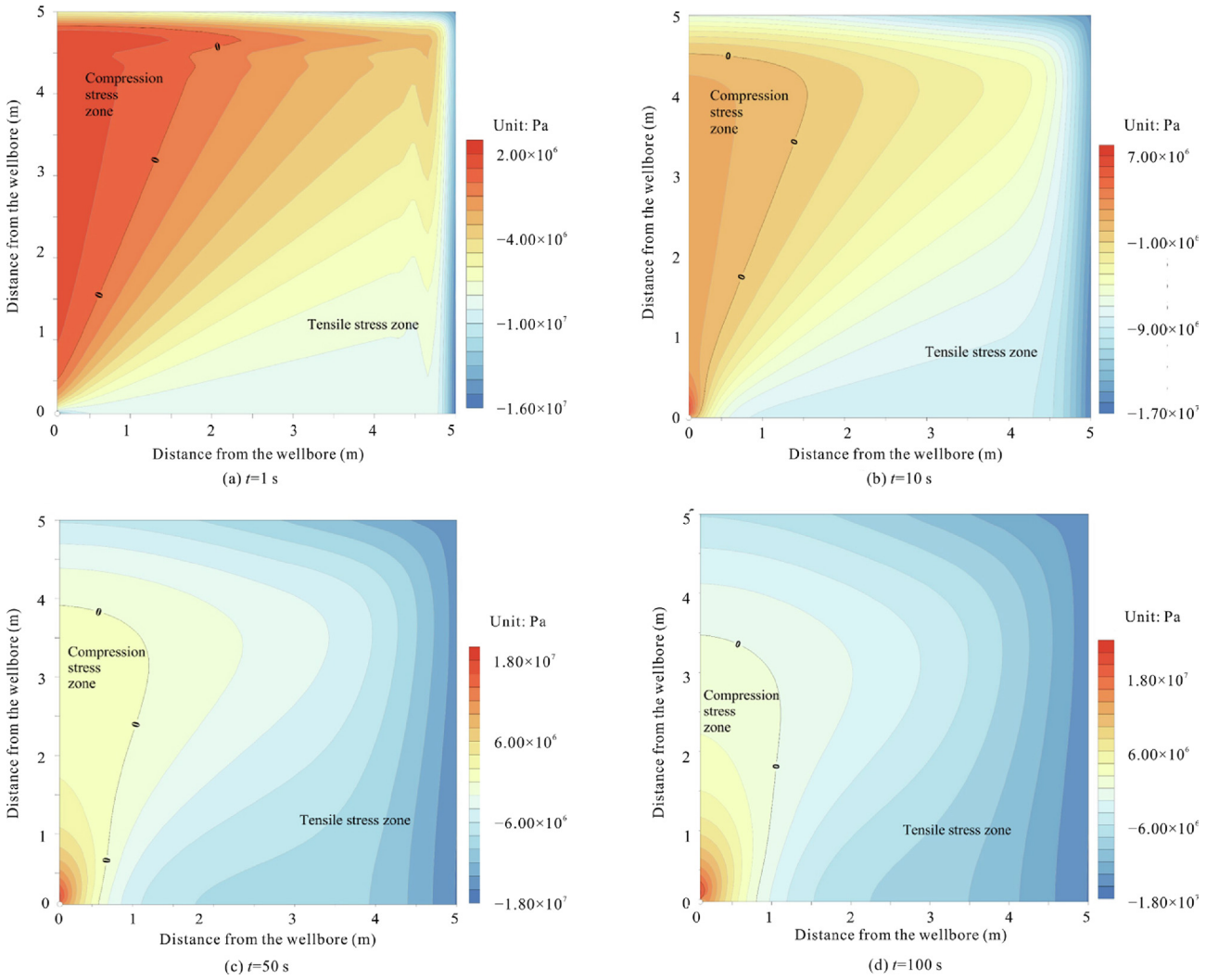

Fig. 6. Distribution of effective shear stress [59].

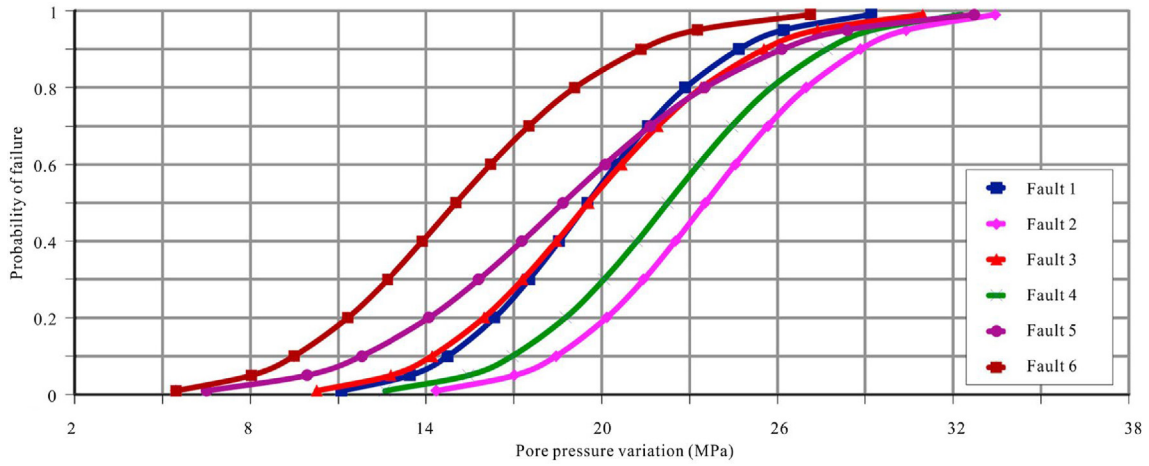

Fig. 7. The probability of fault rupture due to pore pressure variation [62].

tions of CO_2 injection and the geomechanical response(Fig. 9). This includes analyzing the patterns of pore pressure variation due to injection, the consequent changes in rock stress, and the deformation conditions of the geological formation [63]. (2) Accounting for the influence of natural fractures and faults, studies investigate the activation of these features caused by CO_2 injection under THM and THMC coupling processes, as well as their impact on the extent of surface deformation [64].

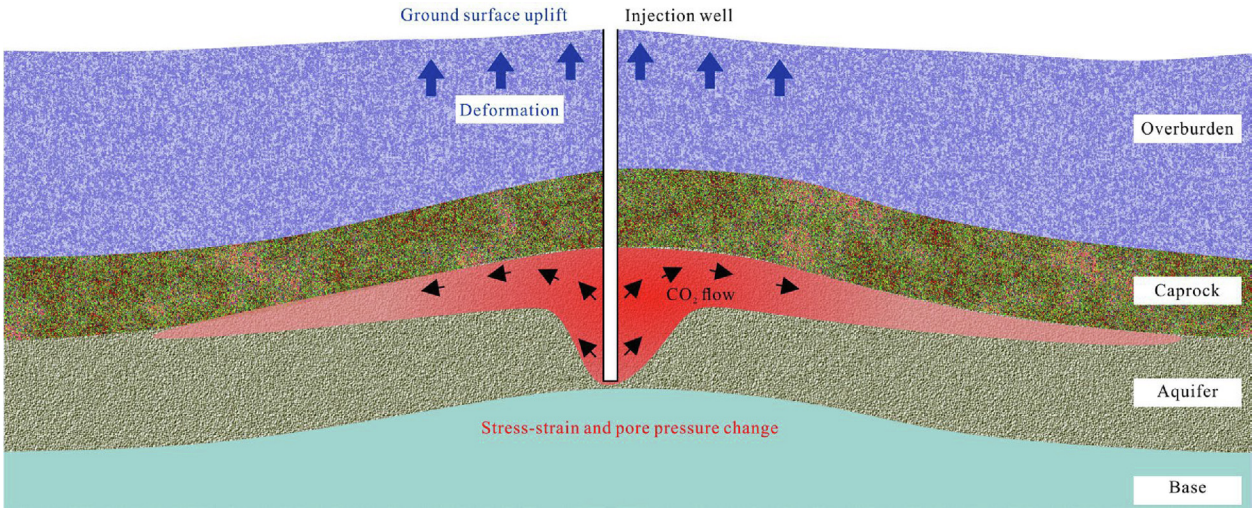

Fig. 8. The surface deformation induced by CO_2 injection and migration (modified after Li et al. [59]).

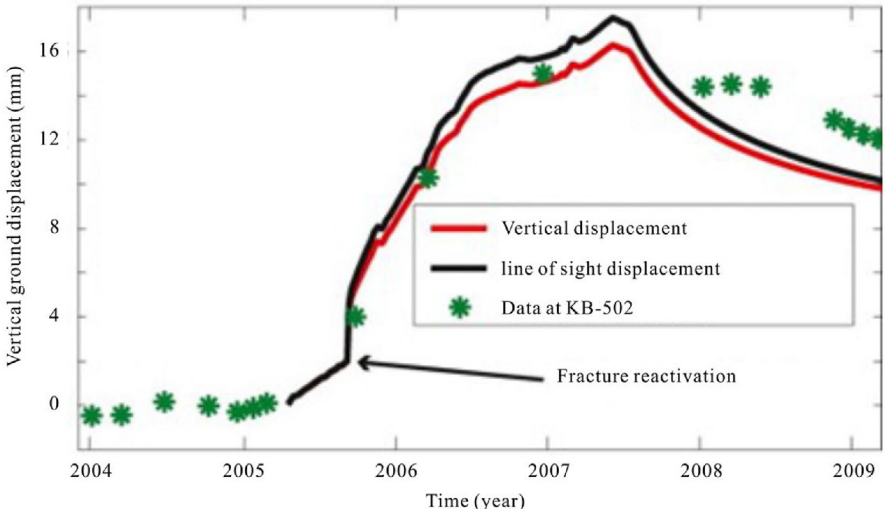

Fig. 9. Numerical simulation results of surface deformation versus measured results (modified after Rinaldi AP et al. [65]).

4.4. CO_2 fracturing simulation

CO_2 fracturing technology is a process that enhances production by using CO_2 as an additive to fracturing fluids or as a proppant-carrying fluid [66]. It can be categorized into CO_2 energized fracturing, CO_2 foam fracturing, and liquid (L-CO_2) or supercritical (SC-CO_2) CO_2 fracturing [67]. The THMC coupling processes involved in CO_2 fracturing include [68]: (1) Reduction in effective stress and induced shear failure caused by thermal stress and pore pressure perturbation (TH-M); (2) Reduction in net pressure of fractures required for fracture propagation due to zero surface tension (H-M); (3) Lowering the critical stress for fracture propagation due to adsorption (C-M); (4) Dynamics of fracture propagation facilitated by local phase transition (HT-M).

$$\Delta\sigma_{\mathrm{hT}} = \frac{\alpha_{\mathrm{T}} E \Delta T \frac{n}{m}}{(1-\nu)\left(1+\frac{n}{m}\right)} \tag{19}$$

$$\Delta\sigma_{\mathrm{HT}} = \frac{\alpha_{\mathrm{T}} E \Delta T}{(1-\nu)\left(1+\frac{n}{m}\right)} \tag{20}$$

where $\Delta\sigma_{\mathrm{hT}}$ and $\Delta\sigma_{\mathrm{HT}}$ are thermal stress in the directions vertical and parallel to the fracture, respectively; α_{T} the thermal expansion coefficient; E the elastic modulus; ΔT the change of temperature; and m and n the lengths of the major and minor axes of the cooling zone, respectively.

Current research on the multi-physics coupling of CO_2 fracturing [69] is focused on the characteristics of initiation pressure changes, characterization of fracture surface morphology, conditions for natural fracture activation, geometric morphology and dimensions of artificial fractures, chemical reactions of rock minerals under CO_2 action, variations in porosity and permeability due to CO_2 action, and changes in rock mechanical properties (Fig. 10).

4.5. CO_2-induced fault activation and earthquakes

Large-scale CO_2 injection increases formation pressure, which may activate faults and even induce small to moderate seismic events [71]. Injection experiments in the Rangely field, Colorado, USA, have shown that fluid injection into the formation raises reservoir pressure (Fig. 11), which consequently induces earthquakes [72]. In Fig. 11a, the solid lines represent numerical simulation results, the squares depict the pressure changes measured during the experiment, the colors indicate the locations of the different wells, the gray bars show the number of earthquakes

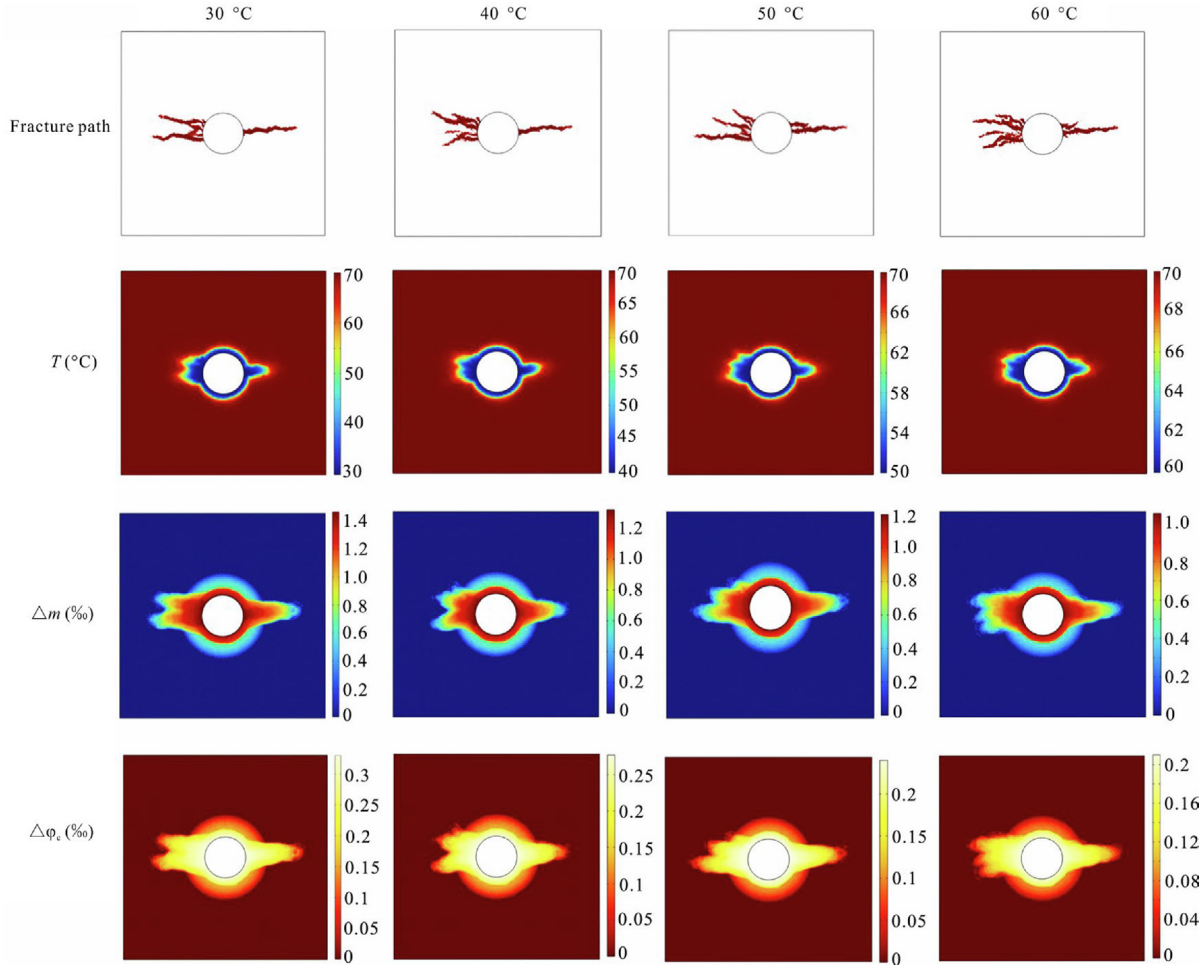

Fig. 10. Final fracture paths, temperature (T), reduction in calcite mass fraction ($\triangle m$), and increase in porosity at different injection temperatures ($\triangle\varphi_c$) [70].

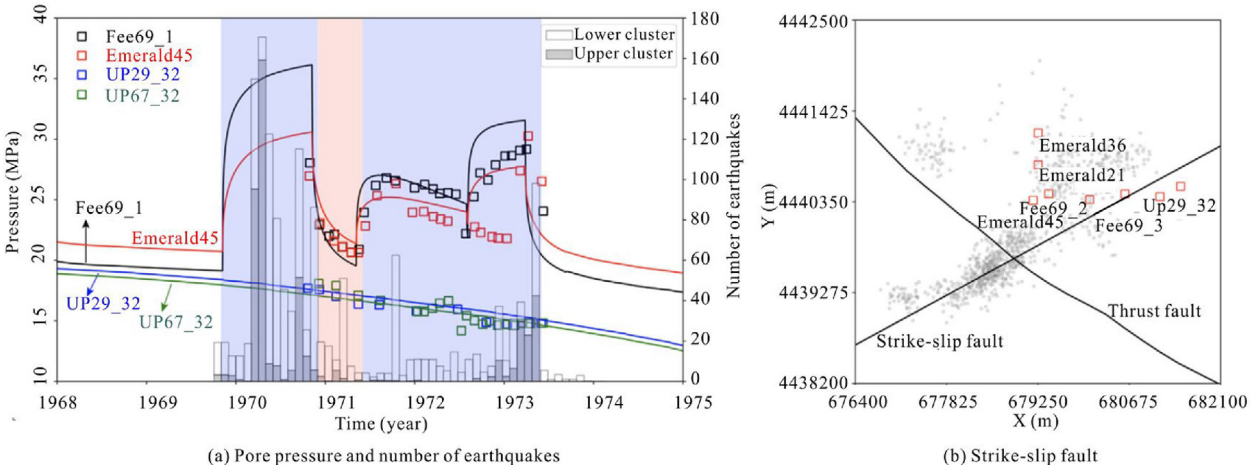

Fig. 11. Stratigraphic pressure variations and seismicity in the injected fluid-induced seismicity experiments in the Rangely field [72].

recorded in the upper cluster, and the white bars represent those in the lower cluster. The blue and red areas correspond to the periods of water injection and extraction, respectively. Fig. 11b's gray circles mark the locations of earthquakes documented during the experiment. This experiment confirms the relationship between fluid pressure and seismic activity [73]. In Japan, the 'Nojima Fault Zone Probe' scientific drilling program observed that seismicity increased significantly four to five days after starting water injections [74], not far from the injection site (Fig. 12), suggesting these earthquakes were likely induced by the water injection [75].

These studies demonstrate that substantial fluid injection into a formation can readily trigger earthquakes. Injecting large vol-

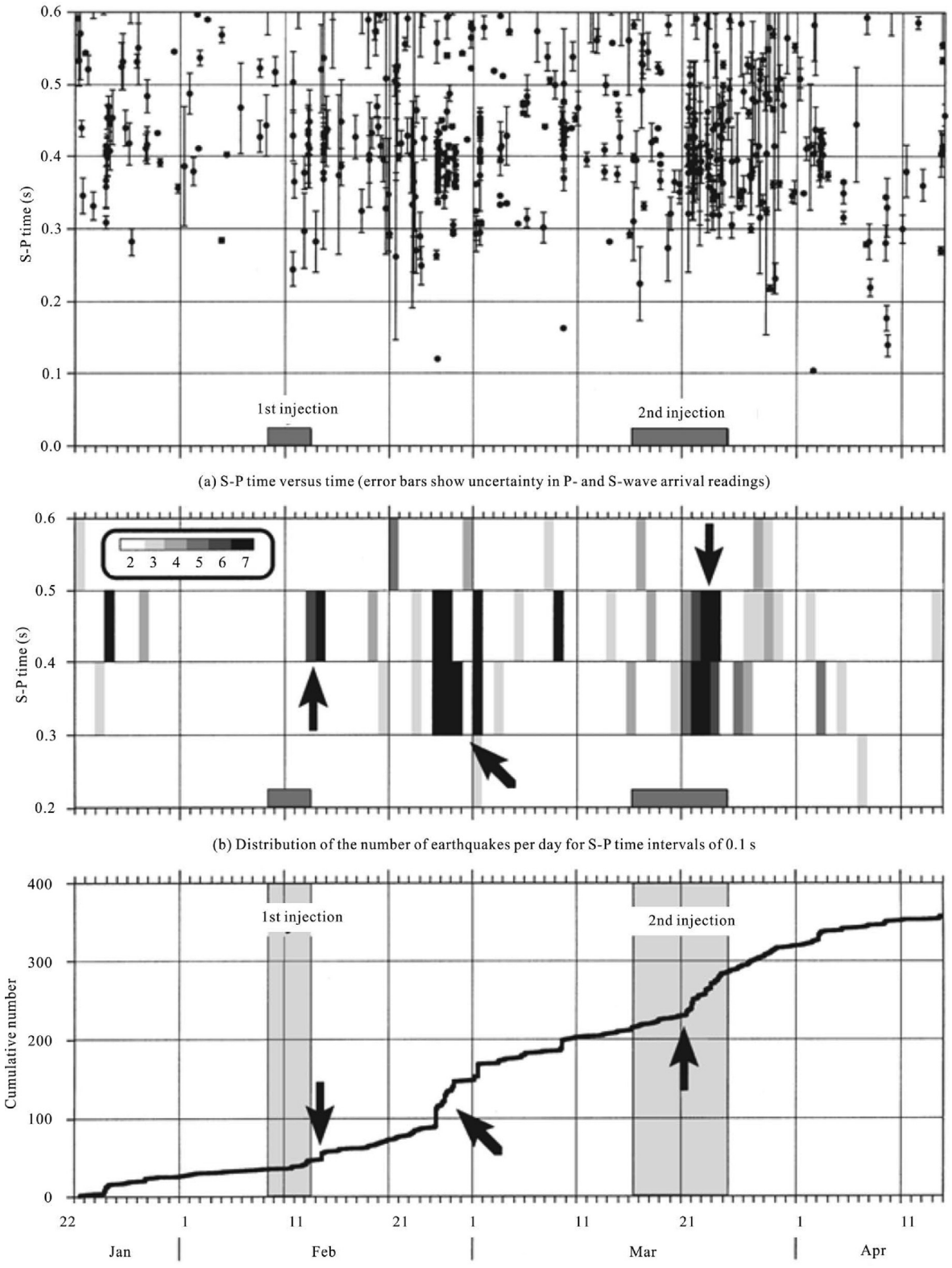

Fig. 12. P- and S-wave arrival times versus fluid injection [75].

umes of CO_2 alters the rock mass's mechanical state [76], and high pore pressures in or near the reservoir can lead to microseismicity [77] or even destructive earthquakes [78]. The primary mechanical mechanism is described by effective stress theory, where injected supercritical CO_2 fluid increases fluid pressure, reducing the effective stress on fault surfaces [79], thereby decreasing shear strength. When the shear strength on the fault surface falls below the shear stress, fault activation

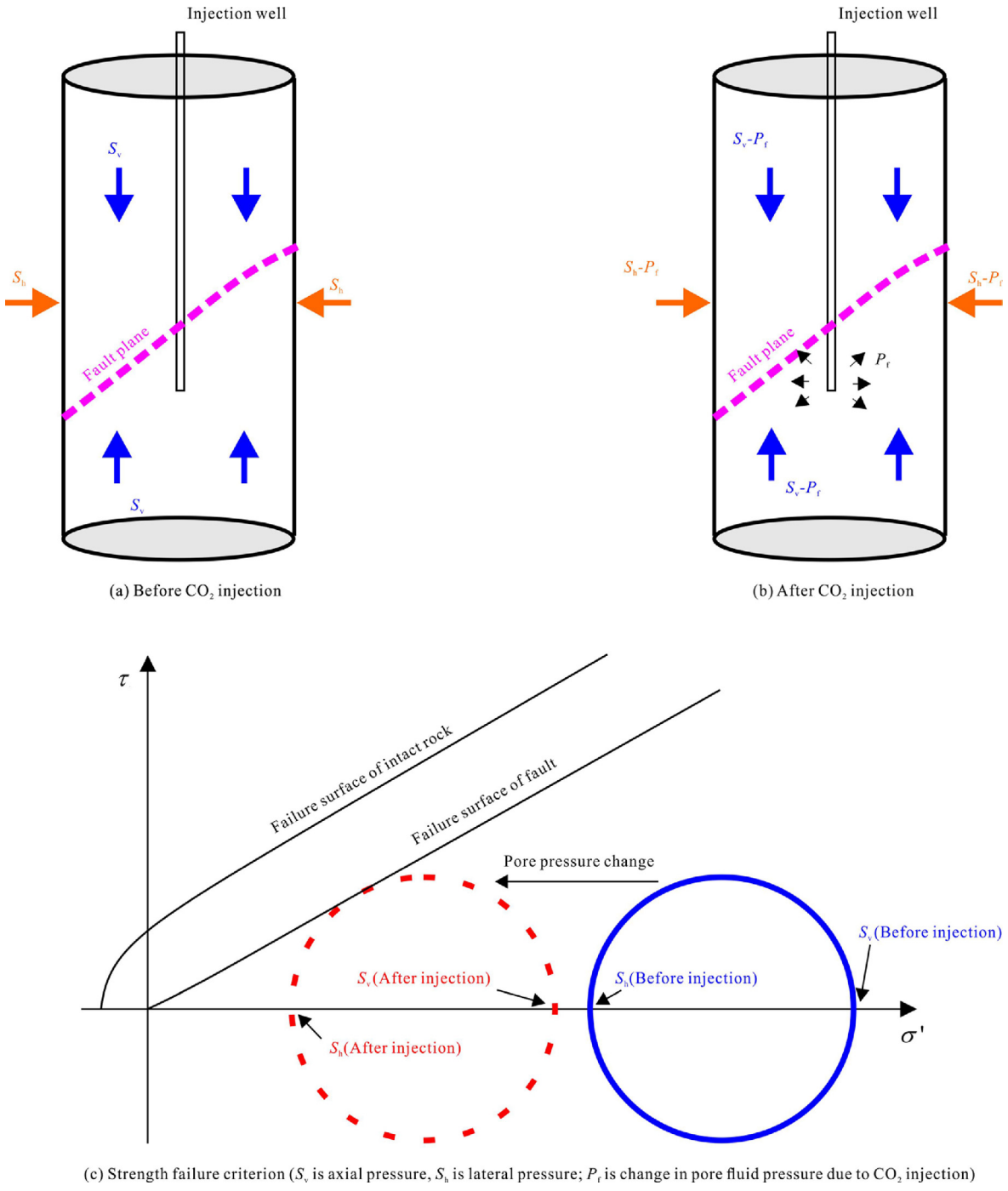

Fig. 13. Plot of fault stability as a function of pore fluid pressure (modified after Streit and Hillis et al. [81]).

and sliding occur, resulting in seismic events [80]. This mechanism is depicted in Fig. 13.

According to the Mohr-Coulomb strength failure criterion, fault activation occurs when the shear stress on the fault surface exceeds the fault's shear strength:

$$|\tau_s| \geqslant c + \sigma'_n \tan\varphi \tag{21}$$

where σ' is the effective stress; τ_s the shear stress; c the cohesion; and φ the angle of internal friction, the values of which are dependent on factors such as temperature, saturation, and mineral composition.

After CO_2 injection, fluid pressure build-up and changes in the temperature field alter the effective stress field, and chemical reactions reduce rock strength. Increased pore pressure causes Mohr's circle to shrink and shift leftward (from (1) to (2) in Fig. 14). The CO_2 temperature is cooler than the reservoir's at the injection well's bottom, cooling the surrounding rock and inducing thermal stress, shifting the state to shear damage (the Mohr's circle labeled as (3) in Fig. 14). Thermal stress depends on temperature difference, volume modulus, and rock matrix volumetric thermal expansion coefficient. The pore pressure change due to temperature can be estimated by the following equation:

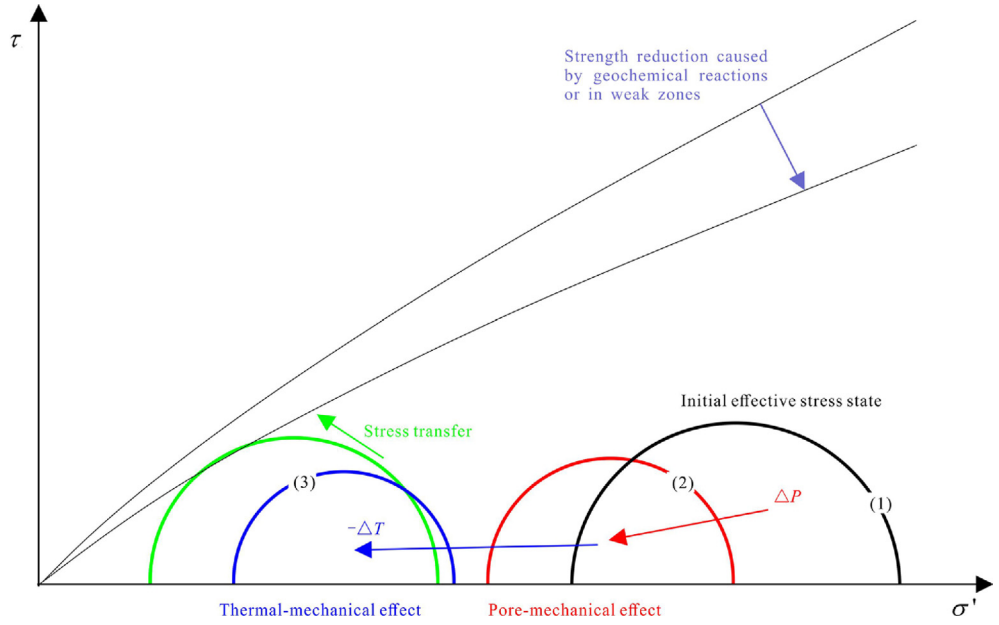

Fig. 14. Schematic diagram of stress state coupling effect (modified after Vilarrasa et al. [82]).

$$\begin{cases} \Delta p = \frac{\alpha}{A}\Delta\varepsilon_V + \frac{1}{A}\Delta\zeta + \frac{\phi\beta_f + (\alpha-\phi)\beta_S^{vol}}{A}\Delta T \\ A = \frac{\phi}{K_f} + \frac{\alpha-\phi}{K_b} \end{cases} \tag{22}$$

where Δp is the change in pore pressure due to temperature change; α the Biot coefficient; A the area;$\Delta\varepsilon_V$ the change in volumetric strain $\Delta\zeta$ the fluid strain; β_f the fluid volumetric coefficient of thermal expansion; β_S^{vol} the rock matrix volumetric coefficient of thermal expansion; ΔT the change in temperature; K_f the fluid bulk modulus; and K_b the rock bulk modulus.

Once the Mohr-Coulomb strength failure criterion indicates fault destabilization, the potential magnitude of induced earthquakes can be predicted [83]:

$$\begin{cases} M_0 = \mu A d \\ M = (\lg M_0/1.5) - 6.1 \end{cases} \tag{23}$$

where M_0 is the energy released by the activation of the fault; M the magnitude; μ the shear modulus of the fault; A the area of the fault destabilization; and d the magnitude of the misalignment displacement.

5. Development directions of THMC coupling

Numerous research achievements have emerged in the areas of coupled THMC mathematical models, numerical solution methods, and on-site applications of multi-physics coupling in the process of CO_2 geological storage and utilization. These findings lay a theoretical foundation and offer a design methodology for construction parameters for on-site CO_2 storage and utilization implementation. Based on the current state of research, the following aspects are still worthy of further exploration:

(1) Constructing constitutive models relevant to CO_2 geological storage and utilization. When investigating caprock integrity using existing elastic and plastic constitutive models, inconsistent results may be obtained: an elastic constitutive model suggests that the mechanical integrity of the caprock is better in the initial tensile stress state (vertical stress greater than horizontal stress) than in the initial compressive stress state (vertical stress less than horizontal stress). However, analyses based on a plastic constitutive model yield diametrically opposite results [84]. Thus, there is an urgent need to develop constitutive models that are suitable for CO_2 geological storage and utilization. These models should more accurately describe the changes in rock properties after CO_2 injection and the effects of injection pressure on the stress–strain-damage characteristics of rocks. Further development of these models is essential to address the shortcomings of existing models and provide theoretical support for the evaluation of caprock integrity.

(2) Building a multi-scale, multi-physics mathematical model with an efficient numerical solution method. CO_2 geological storage and utilization involve the solute transfer and chemical reactions at the micro-scale, rock structure damage at the mesoscale, and macro-scale phenomena such as rock failure and activation of faults and natural fractures. Additionally, geological models encompass features ranging from small fractures at the meter scale to large faults at the kilometer scale. Addressing how to describe the geometric information of fractures and faults while reducing computational costs is a pressing issue [85,86]. By combining equivalent single-porosity models, dual-porosity models, and embedded discrete fracture models, a composite medium model can be constructed, and a corresponding multi-scale, multi-physics mathematical model can be established. Furthermore, employing hybrid discrete methods to construct parallel algorithms in time and space can help reduce the computational burden and enhance computational efficiency.

(3) Developing a specialized THMC coupling simulator for CO_2 geological storage and utilization. The coupled THMC governing equations for CO_2 geological storage and utilization consist of a set of transient, nonlinear partial differential equations, presenting challenges in discretization in time and space, and difficulty in achieving a balance between accuracy, stability, and computational speed. The existing simulator solvers are primarily developed from numerical simulators for oil and gas field projects [87], with some incorporating the geochemical reactions of CO_2-H_2O-rock [88]. However, most simulators only consider simple HM, THM, or THC coupling [89], typically achieving THMC cou-

pling through the combination of multiple simulators [90], which limits the large-scale application of THMC coupling numerical simulations in CO_2 storage and utilization engineering problems. Therefore, there is a need to develop a specialized THMC coupling simulator for CO_2 geological storage and utilization, providing the necessary technical means for solving practical engineering problems.

(4) Numerical simulations for CO_2 geological sequestration and utilization are currently facing breakthrough demands from multidimensional technical challenges. As the scale of sequestration projects expands to kilometer-scale reservoirs, traditional numerical frameworks are increasingly inadequate for high-precision predictions. There is an urgent need to develop large-scale parallel computing systems capable of handling billions of grid cells, which requires optimizing multi-physics data exchange mechanisms under distributed memory architectures and developing explicit–implicit hybrid solvers accelerated by GPUs to balance computational efficiency and numerical stability. At the level of multi-component coupling, it is necessary to overcome the bottleneck of strongly nonlinear interactions across time scales in THMC processes by establishing coupled mathematical models that incorporate mineral dissolution-precipitation kinetics and non-Darcy flow-stress synergy. Additionally, dynamic interface tracking techniques must be advanced to characterize the evolution of CO_2 migration fronts. For the challenge of multi-scale embedding, research is shifting towards pore-core-reservoir cross-scale coupling methods. This involves introducing equivalent constitutive parameters derived from microscale digital rock core simulations to construct surrogate models for the macroscopic geomechanical response, complemented by adaptive grid coarsening techniques to achieve synergistic optimization between local refinement and global computational load. Furthermore, engineering-scale simulations must integrate geostatistical inversion with machine learning-based uncertainty quantification techniques. The development of multi-scenario coupled prediction platforms that consider reservoir heterogeneity and fault activation risks will provide scientific support for assessing the safety of sequestration over million-year time spans. The innovative integration of these technical pathways will drive the substantive transition of THMC coupled simulations from theoretical models to practical engineering decision-making tools.

6. Conclusions

This review systematically summarizes the current advances in THMC coupling modeling for CO_2 geological storage and utilization. The main conclusions are as follows:

(1) The THMC processes are governed by a set of conservation equations, including mass, momentum, and energy conservation, as well as kinetic and equilibrium-based chemical reaction models. Their interdependence determines the evolution of reservoir parameters such as porosity, permeability, and mechanical integrity.

(2) Three principal numerical coupling strategies—fully coupled, iterative coupled, and explicit coupled methods—are critically compared. Their computational characteristics, stability performance, and suitability for heterogeneous reservoir modeling are analyzed, providing a reference framework for method selection under varying simulation scenarios.

(3) Representative simulators (e.g., TOUGH, CMG-GEM, COMSOL, GEOSX) are comparatively reviewed with respect to their coupling mechanisms, governing equation solvers, scalability, and domain-specific applicability. The comparison highlights trade-offs between flexibility, computational efficiency, and engineering applicability.

(4) Major technical challenges include the lack of robust chemo-mechanical constitutive models, limited scalability of current algorithms to high-resolution 3D domains, and insufficient mechanisms for cross-scale parameter transfer. Addressing these gaps requires the development of physics-informed solution schemes, high-performance computing integration, and domain-specific hybrid modeling strategies.

Acknowledgments

This work was supported by the China Postdoctoral Science Foundation (NO. 2024M752803), the National Natural Science Foundation of China (No. 52179112), and the Open Fund of National Key Laboratory of Oil and Gas Reservoir Geology and Exploitation (Southwest Petroleum University) (NO. PLN2023-02).

References

[1] Iea. CO_2 Emissions in 2022. Paris: International Energy Agency; 2023.
[2] Dou LR, Sun LD, Lyu WF, Wang MY, Gao F, Gao M, Jiang H. Trend of global carbon dioxide capture, utilization and storage industry and challenges and countermeasures in China. Petrol Explor Dev 2023;50(5):1246–60.
[3] Zhang NL, Cao B, Liu FS, Jiang LL, Luo ZF, Liu PL, Chen YS. CO_2 flooding effects and breakthrough times in low-permeability reservoirs with injection–production well patterns containing hydraulic fractures. Nat Gas Ind B 2025;12(3):339–55.
[4] Li ZB, Ren T, Cheng YP, He XQ, Qiao M, Black D, Li K, Nemcik J. Study of methane and carbon dioxide adsorption-desorption hysteresis in coals from Sydney Basin: a theoretical and experimental approach. Int J Min Sci Technol 2024;34(10):1453–63.
[5] Li NY, Yu JJ, Zhang HT, Zhang Q, Kang J, Zhang NL, Wang C. Simulation of wellbore temperature and pressure field in supercritical carbon dioxide fracturing. Petrol Sci Technol 2024;42(2):190–210.
[6] Abdullah S, Wang K, Chen XH, Khan A. The impact of thermal transport on reactive THMC model for carbon capture and storage. Geomech Energy Environ 2023;36:100511.
[7] Zhang NL, Liu FS, Jiang LL, Luo ZF, Ju YW, Liu PL, Zhao LQ, Pei YX. Effects of phase-transition heat on fracture temperature in self-propping phase-transition fracturing technology. Petrol Explor Dev 2024;51(6):1587–97.
[8] Yu EY, Di Y, Wu H, Cao XP, Zhang QF, Zhang CB. Numerical simulation on risk analysis of CO_2 geological storage under multi-field coupling: a review. Chin J Theor Appl Mech 2023;55(9):2075–90. In Chinese.
[9] Cheng YX, Liu WN, Xu TF, Zhang YJ, Zhang XW, Xing YY, Feng B, Xia Y. Seismicity induced by geological CO_2 storage: a review. Earth Sci Rev 2023;239:104369.
[10] Eyinla DS, Leggett S, Badrouchi F, Emadi H, Adamolekun OJ, Akinsanpe OT. A comprehensive review of the potential of rock properties alteration during CO_2 injection for EOR and storage. Fuel 2023;353:129219.
[11] Wu Y, Li P. The potential of coupled carbon storage and geothermal extraction in a CO_2-enhanced geothermal system: a review. Geotherm Energy 2020;8(1):19.
[12] Ajayi T, Gomes JS, Bera A. A review of CO_2 storage in geological formations emphasizing modeling, monitoring and capacity estimation approaches. Petrol Sci 2019;16(5):1028–63.
[13] Akono AT, Druhan JL, Dávila G, Tsotsis T, Jessen K, Fuchs S, Crandall D, Shi ZF, Dalton LE, Tkach M, Goodman AL, Frailey S, Werth CJ. A review of geochemical–mechanical impacts in geological carbon storage reservoirs. Greenh Gases Sci Technol 2019;9(3):474–504.
[14] Masoudian MS. Multiphysics of carbon dioxide sequestration in coalbeds: A review with a focus on geomechanical characteristics of coal. J Rock Mech Geotech Eng 2016;8(1):93–112.
[15] Abidoye LK, Khudaida KJ, Das DB. Geological carbon sequestration in the context of two-phase flow in porous media: A review. Crit Rev Environ Sci Technol 2015;45(11):1105–47.
[16] Song J, Zhang DX. Comprehensive review of caprock-sealing mechanisms for geologic carbon sequestration. Environ Sci Technol 2013;47(1):9–22.
[17] Jiang X. A review of physical modelling and numerical simulation of long-term geological storage of CO_2. Appl Energy 2011;88(11):3557–66.

[18] Zhang NL, Luo ZF, Chen ZX, Liu FS, Liu PL, Chen WY, Wu L, Zhao LQ. Thermal–hydraulic–mechanical–chemical coupled processes and their numerical simulation: a comprehensive review. Acta Geotech 2023;18(12):6253–74.
[19] Liu ZY, Liu YG, Li TX, Wei MH. Seepage and heat transfer of dominant flow in fractured geothermal reservoirs: a review and outlook. Water 2023;15(16):2953.
[20] Khandoozi S, Hazlett R, Fustic M. A critical review of CO_2 mineral trapping in sedimentary reservoirs–from theory to application: Pertinent parameters, acceleration methods and evaluation workflow. Earth Sci Rev 2023;244:104515.
[21] Li GS, Ji JY, Song XZ, Shi Y, Li S, Song ZH, Song GF, Xu FQ. Research advances in multi-field coupling model for geothermal reservoir heat extraction. Energy Rev 2022;1(2):100009.
[22] Birkholzer JT, Bond AE. DECOVALEX-2019: An international collaboration for advancing the understanding and modeling of coupled thermo-hydro-mechanical-chemical (THMC) processes in geological systems. Int J Rock Mech Min Sci 2022;154:105097.
[23] Pandey SN, Vishal V, Chaudhuri A. Geothermal reservoir modeling in a coupled thermo-hydro-mechanical-chemical approach: a review. Earth Sci Rev 2018;185:1157–69.
[24] Wang L, Wang SH, Zhang RL, Wang C, Xiong Y, Zheng XS, Li SR, Jin K, Rui ZH. Review of multi-scale and multi-physical simulation technologies for shale and tight gas reservoirs. J Nat Gas Sci Eng 2017;37:560–78.
[25] Li X, Yuan W, Bai B, Liu M, He H. Geomechanical modeling of CO_2 storage in deep saline aquifers-a review. In: ISRM International Symposium Wroclaw: ISRM. p. 79–89.
[26] Rutqvist J, Tsang CF. Multiphysics processes in partially saturated fractured rock: Experiments and models from Yucca Mountain. Rev Geophys 2012;50(3):RG3006.
[27] Xu HR, Liu GH, Zhao ZH, Ma F, Wang GL, Chen YD. Coupled THMC modeling on chemical stimulation in fractured geothermal reservoirs. Geothermics 2024;116:102854.
[28] Yi W, Rao QH, Li Z, Sun DL, Shen QQ. Thermo-hydro-mechanical-chemical (THMC)coupling fracture criterion of brittle rock. Trans Nonferrous Met Soc China 2021;31(9):2823–35.
[29] Luo ZF, Zhang NL, Zhao LQ, Yuan XF, Zhang Y. A novel stimulation strategy for developing tight fractured gas reservoir. Petroleum 2018;4(2):215–22.
[30] Yin SD, Dusseault MB, Rothenburg L. Coupled THMC modeling of CO_2 injection by finite element methods. J Petrol Sci Eng 2011;80(1):53–60.
[31] Fan CJ, Elsworth D, Li S, Zhou LJ, Yang ZH, Song Y. Thermo-hydro-mechanical-chemical couplings controlling CH_4 production and CO_2 sequestration in enhanced coalbed methane recovery. Energy 2019;173:1054–77.
[32] Pei YX, Zhang NL, Zhou HX, Zhang SC, Zhang W, Zhang JH. Simulation of multiphase flow pattern, effective distance and filling ratio in hydraulic fracture. J Petrol Explor Prod Technol 2020;10(3):933–42.
[33] Yin SD, Towler BF, Dusseault MB, Rothenburg L. Fully coupled THMC modeling of wellbore stability with thermal and solute convection considered. Transp Porous Medium 2010;84(3):773–98.
[34] Vilarrasa V, Carrera J, Olivella S. Two-phase flow effects on the CO_2 injection pressure evolution and implications for the caprock geomechanical stability. 3rd European Conference on Unsaturated Soils. Paris: E3S Web Conf, 2016.
[35] Hao JC, Wen H, Ma L, Fei JB, Ren LF. Theoretical derivation of a prediction model for CO_2 adsorption by coal. ACS Omega 2021;6(20):13275–83.
[36] Guo W, Hu ZM, Zuo L, Gao SS, Yu RZ, Zeng B. Gas desorption: Diffusion: Seepage coupled experiment of shale matrix and mathematic model. Chin J Theor Appl Mech 2015;47(6):916–22. In Chinese.
[37] Zhang NL, Chen ZX, Luo ZF, Liu PL, Chen WY, Liu FS. Effect of the phase-transition fluid reaction heat on wellbore temperature in self-propping phase-transition fracturing technology. Energy 2023;265:126136.
[38] Zhang RL, Xiong Y, Winterfeld PH, Yin XL, Wu YS. A novel computational framework for thermal-hydrological-mechanical-chemical processes of CO_2 geological sequestration into a layered saline aquifer and a naturally fractured enhanced geothermal system. Greenh Gases Sci Technol 2016;6(3):370–400.
[39] Black JR, Carroll SA, Haese RR. Rates of mineral dissolution under CO_2 storage conditions. Chem Geol 2015;399:134–44.
[40] Zhang RL, Winterfeld PH, Yin XL, Xiong Y, Wu YS. Sequentially coupled THMC model for CO_2 geological sequestration into a 2D heterogeneous saline aquifer. J Nat Gas Sci Eng 2015;27:579–615.
[41] Cai GQ, Zhao CG, Liu Y, Li J. Volume change behavior of unsaturated soils under non-isothermal conditions. Chin Sci Bull 2011;56(23):2495–504.
[42] Wilkins A, Green CP, Ennis-King J. An open-source multiphysics simulation code for coupled problems in porous media. Comput Geosci 2021;154:104820.
[43] Ma Y, Chen XH, Hosking LJ, Yu HS, Thomas HR. THMC constitutive model for membrane geomaterials based on Mixture Coupling Theory. Int J Eng Sci 2022;171:103605.
[44] Guo JC, He SG, Deng Y, Zhao ZH. New stress and initiation model of hydraulic fracturing based on nonlinear constitutive equation. J Nat Gas Sci Eng 2015;27:666–75.
[45] Zhong SY, Li T, Liao SF, Fu H, Ma QP. A viscoelastic-plastic constitutive model for mechanical response of plastic-bonded explosive. Int J Solids Struct 2025;320:113466.
[46] Kanfar MF, Chen Z, Rahman SS. Analyzing wellbore stability in chemically-active anisotropic formations under thermal, hydraulic, mechanical and chemical loadings. J Nat Gas Sci Eng 2017;41:93–111.
[47] Sun LN, Zhang Y, Qin Z, Wang TF, Zhang S. A damage constitutive model of rock under hydrochemical cyclic invasion. Adv Civ Eng 2020;2020(1):8842458.
[48] Pan JL, Zhang Y, Li P, Wu X, Xi X. Mechanical properties and thermo-chemical damage constitutive model of granite subjected to thermal and chemical treatments under uniaxial compression. Constr Build Mater 2023;390:131755.
[49] Ren L, Su YL, Zhan SY, Meng FK, Zhao GY. Fully coupled fluid-solid numerical simulation of stimulated reservoir volume (SRV)-fractured horizontal well with multi-porosity media in tight oil reservoirs. J Petrol Sci Eng 2019;174:757–75.
[50] Wang JW, Guo TK, Chen M, Qu ZQ, Liu XQ, Wang XD, Yu MQ. Numerical study of the fracture propagation mechanism of staged methane deflagration fracturing for horizontal wells in shale gas reservoirs. Geoenergy Sci Eng 2023;230:212209.
[51] Larion Y, Zlotnik S, Massart TJ, Díez P. Building a certified reduced basis for coupled thermo-hydro-mechanical systems with goal-oriented error estimation. Comput Mech 2020;66(3):559–73.
[52] Zhang NL, Liu FS, Jiang LL, Mo PQ, Xiao JW, Song Q, Luo YH. Coupled THMC model-based prediction of hydraulic fracture geometry and size under self-propping phase-transition fracturing. Int J Coal Sci Technol 2024;11(1):78.
[53] Soltanian MR, Hajirezaie S, Hosseini SA, Dashtian H, Amooie MA, Meyal A, Ershadnia R, Ampomah W, Islam A, Zhang XY. Multicomponent reactive transport of carbon dioxide in fluvial heterogeneous aquifers. J Nat Gas Sci Eng 2019;65:212–23.
[54] Hao Y, Smith MM, Carroll SA. Multiscale modeling of CO_2-induced carbonate dissolution: from core to meter scale. Int J Greenh Gas Contr 2019;88:272–89.
[55] Li B, Yu H, Xu WL, Huang HW, Huang MC, Meng SW, Liu H, Wu HA. A multi-physics coupled multi-scale transport model for CO_2 sequestration and enhanced recovery in shale formation with fractal fracture networks. Energy 2023;284:129285.
[56] You JY, Ampomah W, Sun Q. Development and application of a machine learning based multi-objective optimization workflow for CO_2-EOR projects. Fuel 2020;264:116758.
[57] Tatomir A, Tomac I, Sauter M. A parametric sensitivity study on CO2 injection in deep saline aquifers accounting for hydro-mechanical microfracturing. In: Energy Geotechnics. Boca Raton: CRC Press; 2016. p. 223–30.
[58] Wang JG, Wang HM, Wang XL, Yang SQ, Wu HT, Leung CF, Tian JL. A multiphysical-geochemical coupling model for caprock sealing efficiency in CO_2 geosequestration. Deep Undergr Sci Eng 2023;2(2):188–203.
[59] Li XC, Li Q, Bai B, Wei N, Yuan W. The geomechanics of Shenhua carbon dioxide capture and storage (CCS) demonstration project in Ordos Basin. China J Rock Mech Geotech Eng 2016;8(6):948–66.
[60] Khan S, Khulief YA, Al-Shuhail AA. Integrated geomechanical and fault activation modeling of the wasia reservoir: a study focused on ground uplift, stability analysis, and CO_2 leakage. In: Planning a Resilient Future along America's Freshwaters - Selected Papers from the World Environmental and Water Resources Congress 2021. San Francisco: American Society of Civil Engineers; 2021. p. 694–707.
[61] Lee J, Min KB, Rutqvist J. Probabilistic analysis of fracture reactivation associated with deep underground CO_2 injection. Rock Mech Rock Eng 2013;46(4):801–20.
[62] Pereira FLG, Roehl D, Paulo Laquini J, Oliveira MFF, Costa AM. Fault reactivation case study for probabilistic assessment of carbon dioxide sequestration. Int J Rock Mech Min Sci 2014;71:310–9.
[63] Zhu QL, Zuo DJ, Zhang SL, Zhang YT, Wang YS, Wang LL. Simulation of geomechanical responses of reservoirs induced by CO_2 multilayer injection in the Shenhua CCS project. China Int J Greenh Gas Contr 2015;42:405–14.
[64] Bao J, Hou ZS, Fang YL, Ren HY, Lin G. Uncertainty quantification for evaluating the impacts of fracture zone on pressure build-up and ground surface uplift during geological CO_2 sequestration. Greenh Gases Sci Technol 2015;5(3):254–67.
[65] Rinaldi AP, Rutqvist J. Modeling of deep fracture zone opening and transient ground surface uplift at KB-502 CO_2 injection well, in Salah. Algeria Int J Greenh Gas Contr 2013;12:155–67.
[66] Wang M, Huang K, Xie WD, Dai XG. Current research into the use of supercritical CO_2 technology in shale gas exploitation. Int J Min Sci Technol 2019;29(5):739–44.
[67] Wang XZ, Wu JQ, Zhang JT. Application of CO_2 fracturing technology for terrestrial shale gas reservoirs. Nat Gas Ind 2014;34(1):64–7. In Chinese.
[68] Feng YX, Firoozabadi A. Phase-field simulation of hydraulic fracturing by CO_2 and water with consideration of thermoporoelasticity. Rock Mech Rock Eng 2023;56(10):7333–55.
[69] Li MK, Ni HJ, Wang RH, Song WQ. The effect of thermal stresses on the relation between rock failure and temperature and pressure of supercritical carbon dioxide jet. Greenh Gases Sci Technol 2018;8(2):218–37.
[70] Wu L, Hou ZM, Xie YC, Luo ZF, Xiong Y, Cheng L, Huang LC. Fracture initiation and propagation of supercritical carbon dioxide fracturing in calcite-rich shale: a coupled thermal-hydraulic-mechanical-chemical simulation. Int J Rock Mech Min Sci 2023;167:105389.
[71] Chen T, Huang LJ. Seismicity characterization around the Farnsworth field site for combined large-scale CO_2 storage and EOR. Int J Greenh Gas Contr 2015;33:63–8.
[72] Silva JA, Byrne H, Plesch A, Shaw JH, Juanes R. Revisiting the classical experiment in earthquake control at the rangely oil field, Colorado, 1970, using a coupled flow and geomechanical model. Bull Seismol Soc Am 2021;111(6):3136–59.
[73] Raleigh CB, Healy JH, Bredehoeft JD. An experiment in earthquake control at rangely. Colorado Sci. 1976;191(4233):1230–7.

[74] Tadokoro K, Ando M, Nishigami K. Induced earthquakes accompanying the water injection experiment at the Nojima fault zone, Japan: Seismicity and its migration. J Geophys Res Solid Earth 2000;105(B3):6089–104.
[75] Tadokoro K, Nishigami K, Ando M, Hirata N, Iidaka T, Hashida Y, Shimazaki K, Ohmi S, Kano Y, Koizumi M, Matsuo S, Wada H. Seismicity changes related to a water injection experiment in the Nojima Fault Zone. Isl Arc 2001;10(3–4):235–43.
[76] Rinaldi AP, Jeanne P, Rutqvist J, Cappa F, Guglielmi Y. Effects of fault-zone architecture on earthquake magnitude and gas leakage related to CO_2 injection in a multi-layered sedimentary system. Greenh Gases Sci Technol 2014;4(1):99–120.
[77] Yang DX, Zhang LZ. Carbon dioxide leakages through fault zones: Potential implications for the long-term integrity of geological storage sites. Aerosol Air Qual Res 2021;21(12):210220.
[78] Niyogi S, Ghosh A, Kumar A, Hammack RW. Tremor signals during fluid injection are generated by fault slip. Science 2023;381(6657):553–8.
[79] Li GM, Qiao XJ. Factors influencing the safety of CO_2 geological storage in deep saline aquifers. Environ Eng Manag J 2014;13(12):2917–28.
[80] Zoback MD, Gorelick SM. To prevent earthquake triggering, pressure changes due to CO_2 injection need to be limited. PNAS 2015;112(33):E4510.
[81] Streit JE, Hillis RR. Estimating fault stability and sustainable fluid pressures for underground storage of CO_2 in porous rock. Energy 2004;29(9–10):1445–56.
[82] Vilarrasa V, Ramírez J, Olivella S, Rutqvist J, Laloui L. Induced seismicity in geologic carbon storage. Solid Earth Discuss 2019;10:1–42.
[83] Cappa F, Rutqvist J. Impact of CO_2 geological sequestration on the nucleation of earthquakes. Geophys Res Lett 2011;38(17):L17313.
[84] Rutqvist J, Birkholzer J, Cappa F, Tsang CF. Estimating maximum sustainable injection pressure during geological sequestration of CO_2 using coupled fluid flow and geomechanical fault-slip analysis. Energy Convers Manag 2007;48(6):1798–807.
[85] Tian W, Huang JJ, Jiang Y, Chen RL. A parallel scalable domain decomposition preconditioner for elastic crack simulation using XFEM. Int J Numer Meth Eng 2022;123(15):3393–417.
[86] Lu XY, Jordan KE, Wheeler MF, Pyzer-Knapp EO, Benatan M. Bayesian optimization for field-scale geological carbon storage. Engineering 2022;18:96–104.
[87] Class H, Ebigbo A, Helmig R, Dahle HK, Nordbotten JM, Celia MA, Audigane P, Darcis M, Ennis-King J, Fan YQ, Flemisch B, Gasda SE, Jin M, Krug S, Labregere D, Naderi A, Pawar R, Sbai MA, Thomas SG, Laurent T, Wei LL. A benchmark study on problems related to CO_2 storage in geologic formations. Comput Geosci 2009;13(4):409–34.
[88] Xu TF, Sonnenthal E, Spycher N, Pruess K. TOUGHREACT: A simulation program for non-isothermal multiphase reactive geochemical transport in variably saturated geologic media: applications to geothermal injectivity and CO_2 geological sequestration. Comput Geosci 2006;32(2):145–65.
[89] Lee DH, Jang H, Cho HH, Hwang J, Kim JW. Improvement on coupling technique between COMSOL and PHREEQC for the reactive transport simulation. J Nucl Fuel Cycle Waste Technol JNFCWT 2023;21(1):175–82.
[90] Zhang GR, Lu P, Zhang YL, Tu K, Zhu C. SupPhreeqc: A program for generating customized Phreeqc thermodynamic datasets from Supcrtbl and extending calculations to elevated pressures and temperatures. Comput Geosci 2020;143:104560.